Probing the dynamics of star-forming regions with far-infrared and submillimeter polarimetry

Simon Coudé

East Asian Observatory

May 1st, 2019

The Perseus molecular cloud complex

Credit: Lynn Hillborn, “*amateur*” astronomer – Grafton, Ontario, Canada

Summary

1. Fundamental principles
   - Dust polarization and magnetic fields
2. Far-Infrared and submillimeter polarimetry
   - BISTRO, HAWC+, BLAST-TNG, ALMA
3. Dynamics of star-forming regions
   - Magnetic field structures in nearby molecular clouds
   - Magnetic and turbulent properties
4. Dust polarization and alignment mechanisms
   - Testing Radiative Alignment Torques (RATs)

1. Fundamental Principles

Messier 16
Credit: NASA/ESA

Molecular Clouds

- Composition
  - Atomic gas
    - Neutral : HI gas
    - Ionized : HII regions
  - Molecular gas
    - H_2, CO, NH_3, …
  - Interstellar dust
    - $\sim 1\ \%$ of the mass
    - Extinction in the optical
    - Formation of molecules
- Star-forming regions
  - Dense and cold environments

Left: Composite image of the Orion nebula – **Salji+ 2015**

A Few Star Formation Criteria

Step 1: Interstellar Cloud

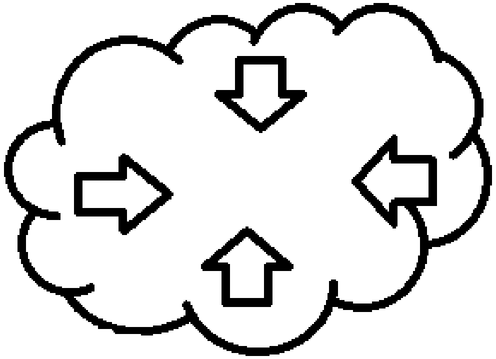

Step 2: ??????

Step 3: Stars!!!!!!!

$$M_{\mathrm{J}} = \left(\frac{5\,k_B \boldsymbol{T}}{G\,\mu m_H}\right)^{\frac{3}{2}} \left(\frac{3}{4\pi\,\boldsymbol{\rho}}\right)^{\frac{1}{2}}$$

Jeans Mass

- ρ is the density of the gas
- T is its temperature

$$t_{ff} = \left(\frac{3\pi}{32\,G\,\boldsymbol{\rho}}\right)^{\frac{1}{2}}$$

Free-Fall Time

$$M_{\Phi} = \sqrt{\frac{5}{3}} \left(\frac{\boldsymbol{\Phi_B}}{3\pi\sqrt{G}}\right)$$

Critical Magnetic Mass

- Φ_B is the magnetic flux

Dust Thermal Emission

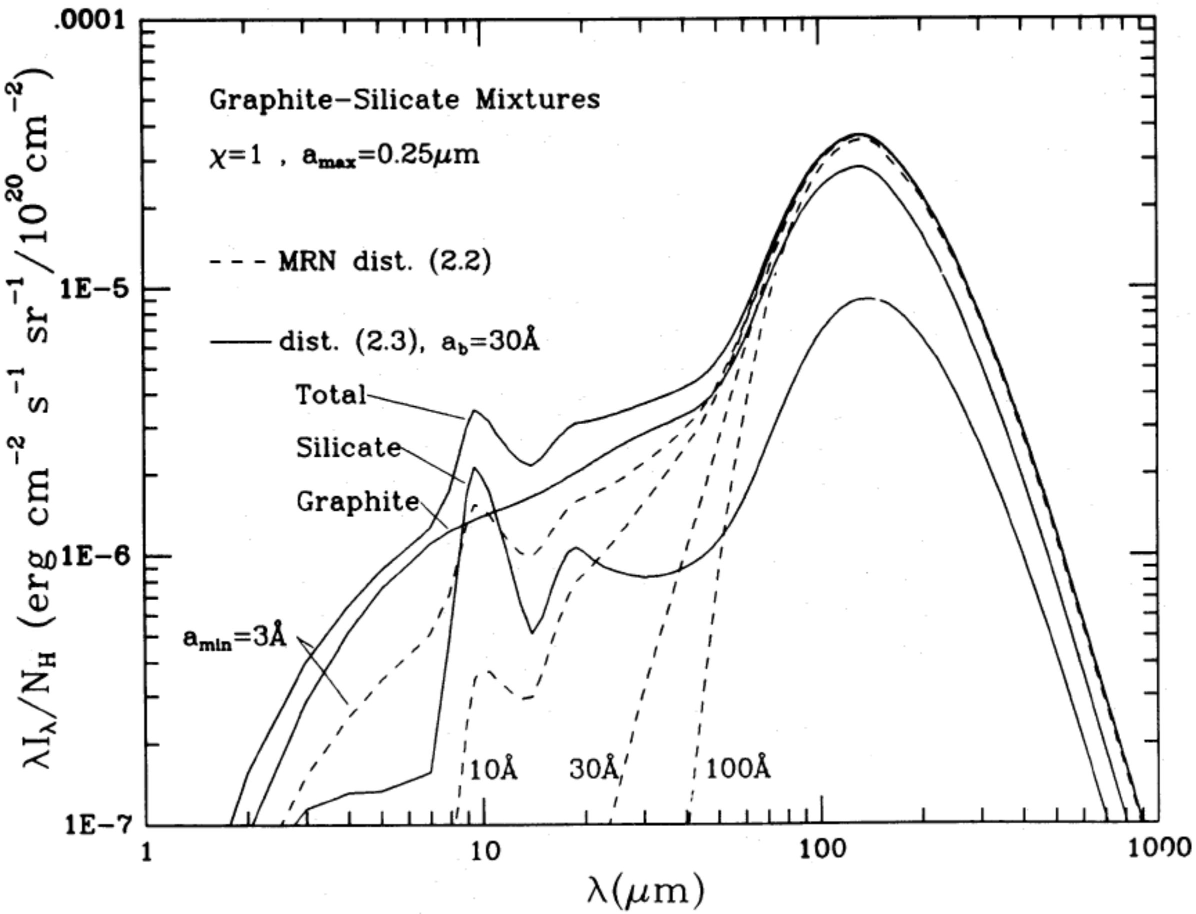

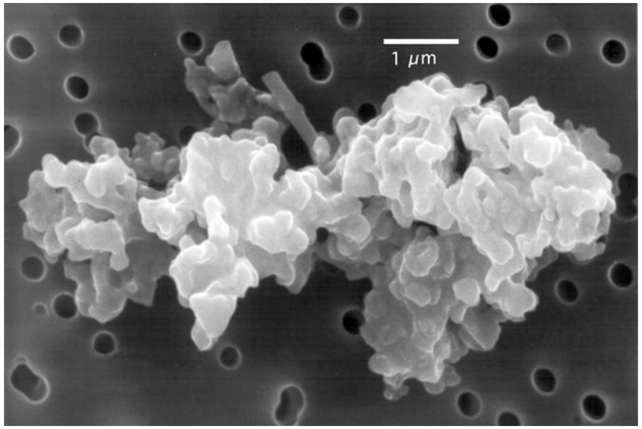

Above: Dust grain Credit: Brownlee & Jessberger

Left: Model from **Draine & Anderson 1985**

- Grain composition
  - Silicates, graphite, PAHs, etc.
  - **Draine & Lee 1984**
- Size distribution and emissivity
  - **MRN 1977**
- **Temperature, density**

Polarization of Dust Thermal Emission

Lazarian & Hoang 2011;
Andersson, Lazarian & Vaillancourt 2015

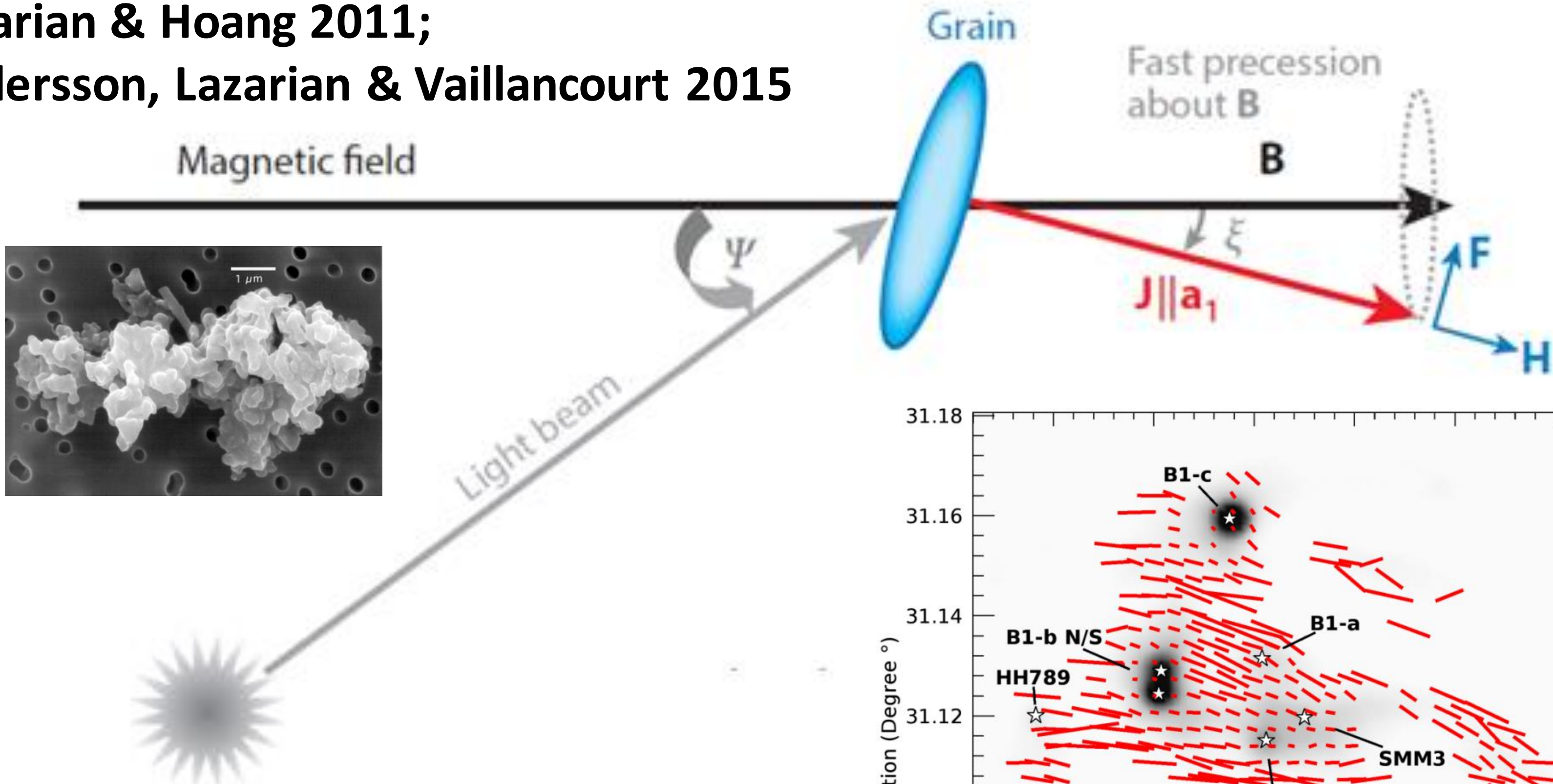

Alignment by Radiative Torques (RAT)

- **Asymmetrical** dust grains
- Interstellar radiation field
- **Lazarian & Hoang 2007**

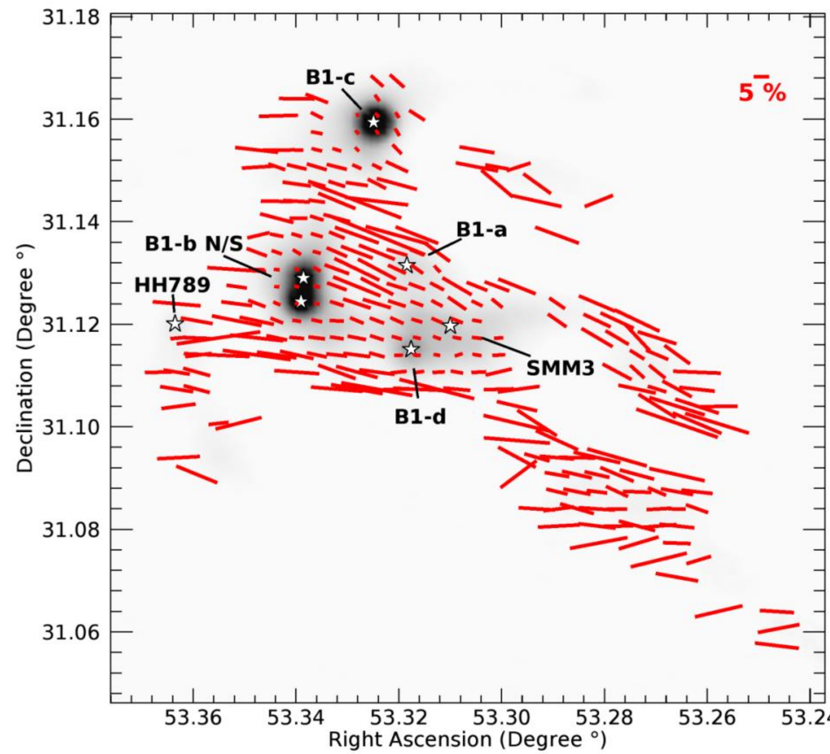

<u>Above</u>: POL-2 polarization in B1

The Davis-Chandrasekhar-Fermi Method

$$B_{pos} = Q\sqrt{4\pi\rho}\,\frac{\delta V}{\delta\theta} \approx 9.3\,\frac{\sqrt{n(H_2)}\,\Delta V}{\delta\theta}\ \mu G$$

Above: Equation from **Crutcher+ 2004**, adapted from **C&F 1953**

- ρ is the **density** of the gas
- δV is the **velocity** dispersion of the gas
- $\delta\theta$ is the dispersion of **polarisation angles**
- Q is the theoretical correction factor (~ 0.5)

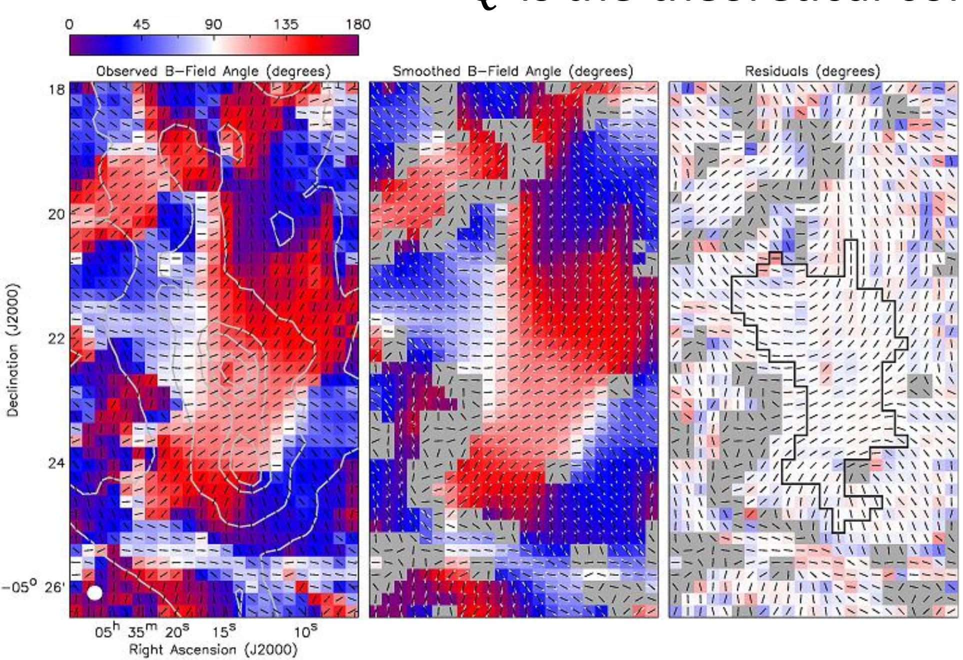

Left: Plane-of-sky magnetic field in OMC-1 from **Pattle+ 2017**

- Difference between vector orientation and smoothed field
- Updated DCF method
- Highly ordered field geometry

Magnetic Fields and Filaments

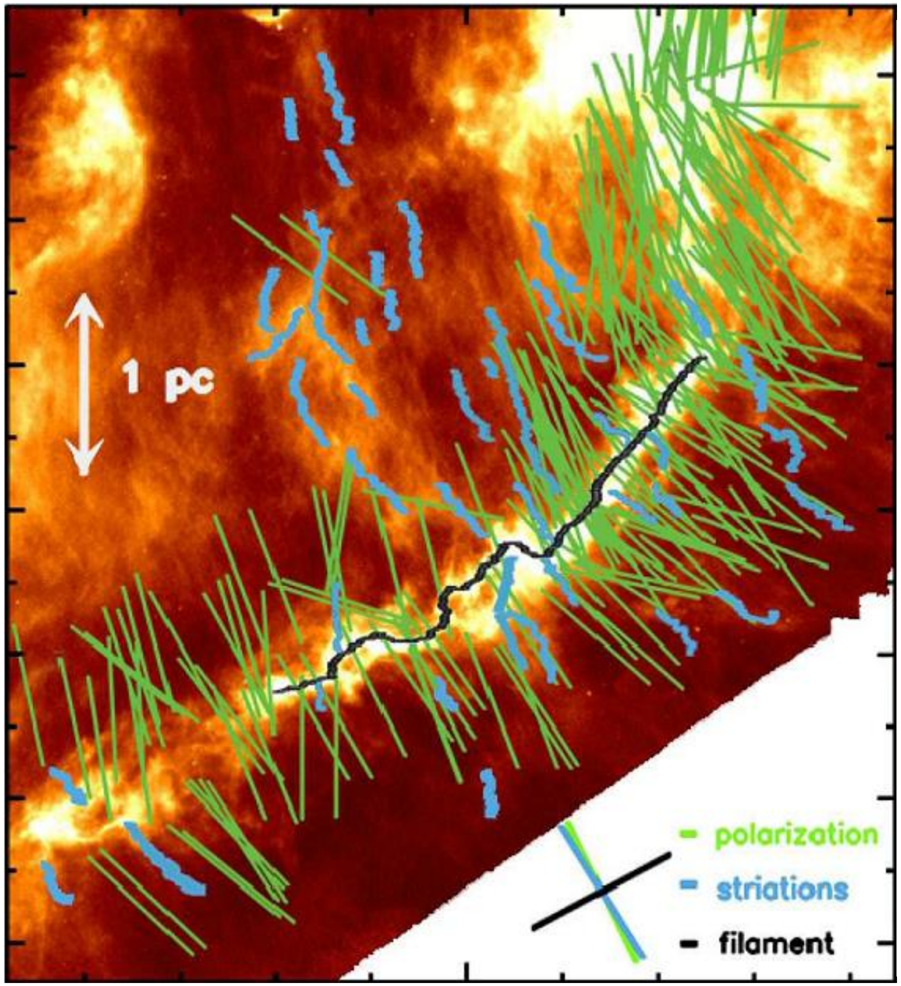

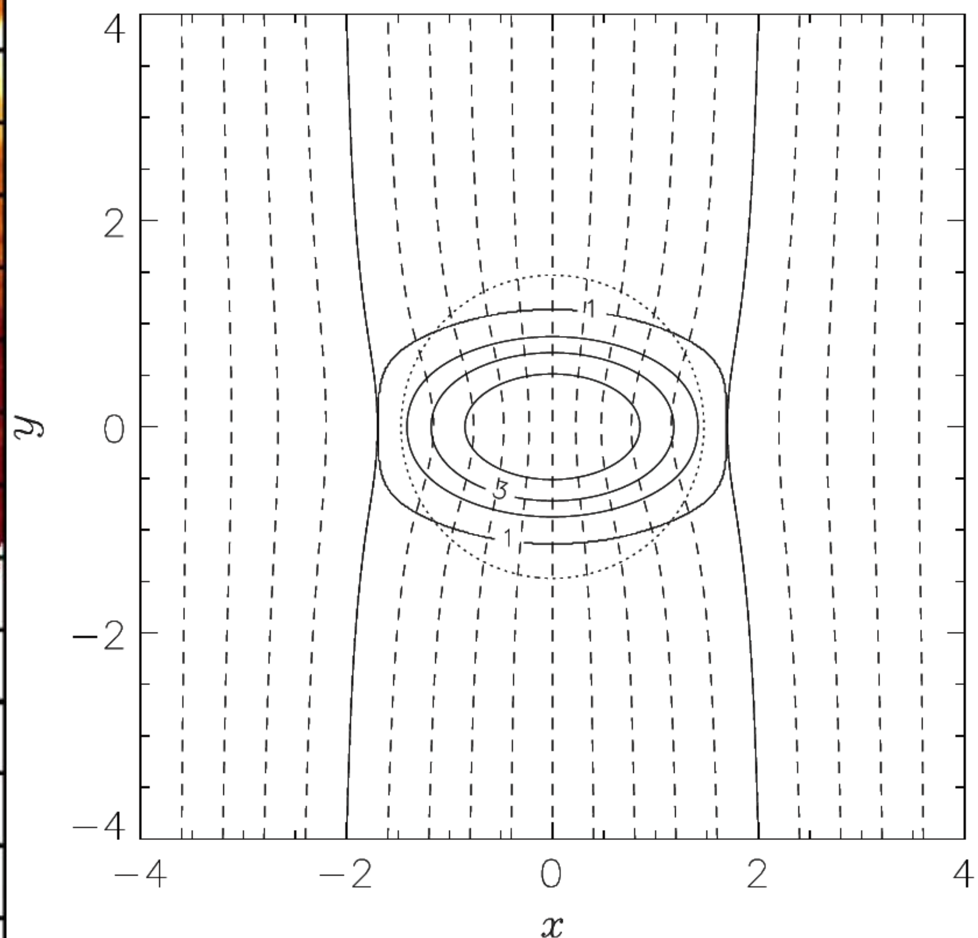

Left: Plane-of-sky magnetic field in Taurus relative to filaments and sub-filaments **André+ 2014**

Right: Magnetohydrostatic filament Model from **Tomisaka 2015**

Magnetic Fields in Protostellar Cores

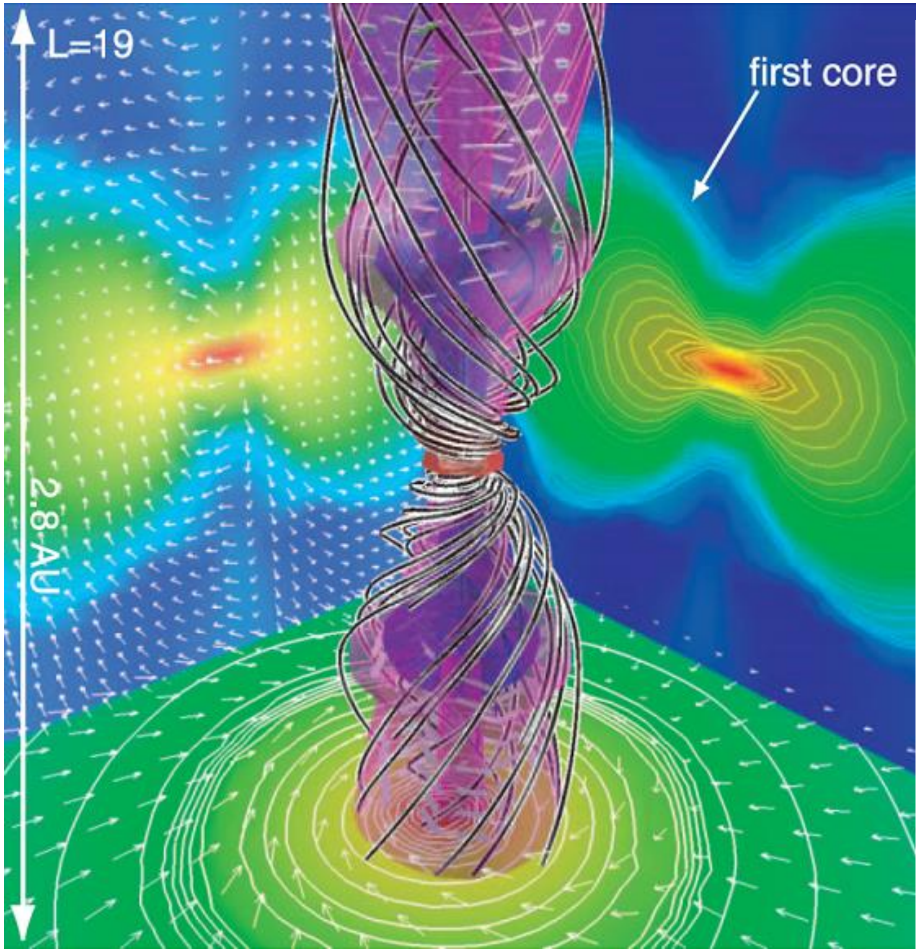

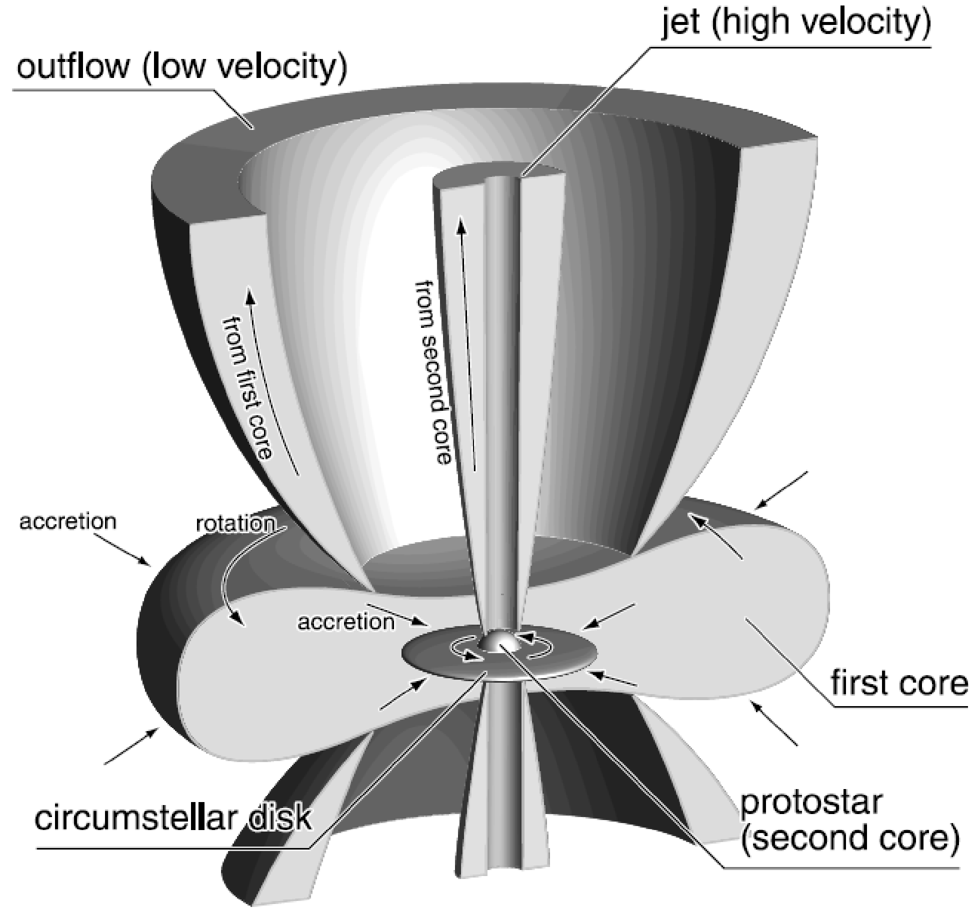

Left: Magnetohydrodynamic simulation of a protostellar outflow and jet
Machida, Inutsuka & Matsumoto 2008

Right: Structure of a protostellar core
Machida, Inutsuka & Matsumoto 2008

Important Questions

- In which regime, if any, can magnetic fields counteract gravitational collapse?
- At what stage, and scale, are magnetic fields in cores decoupled from those in filaments?
- What are the optimal conditions for Radiative Alignment Torques (RATs) in star-forming regions?

2. Far-Infrared and Submillimeter Polarimetry

SOFIA
Credit: NASA

The James Clerk Maxwell Telescope

- Submillimetre observatory
  - Continuum – SCUBA-2
  - Polarimetry – POL-2
  - Spectroscopy – HARP ++
- 15-m single-dish telescope
  - 7.9'' FWHM at 450 μm
  - 13.0'' FWHM at 850 μm
  - Spatial scales up to $\sim 5'$
    - *Experiences may vary*
- Mauna Kea observatory
  - 4092 m in elevation
  - > 50 % of time below $\tau_{225} = 0.12$ (Grade 4)

<u>Left</u>: The JCMT without its wind blind
Credit: East Asian Observatory

BISTRO

B-fields **I**n **ST**ar-forming **R**egi**O**ns

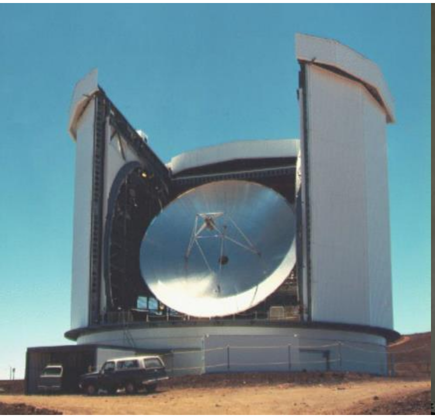

Left: James Clerk Maxwell Telescope
Right: The POL-2 polarimeter

Principal **I**nvestigators:

- **Derek Ward-Thompson** – *UK*
- **Shih-Ping Lai** – *Taiwan*
- **Keping Qiu** – *China*
- **Woojin Kwon** – *Korea*
- **Tetsuo Hasegawa** – *Japan*
- **Pierre Bastien** – *Canada*

And over 100 members !

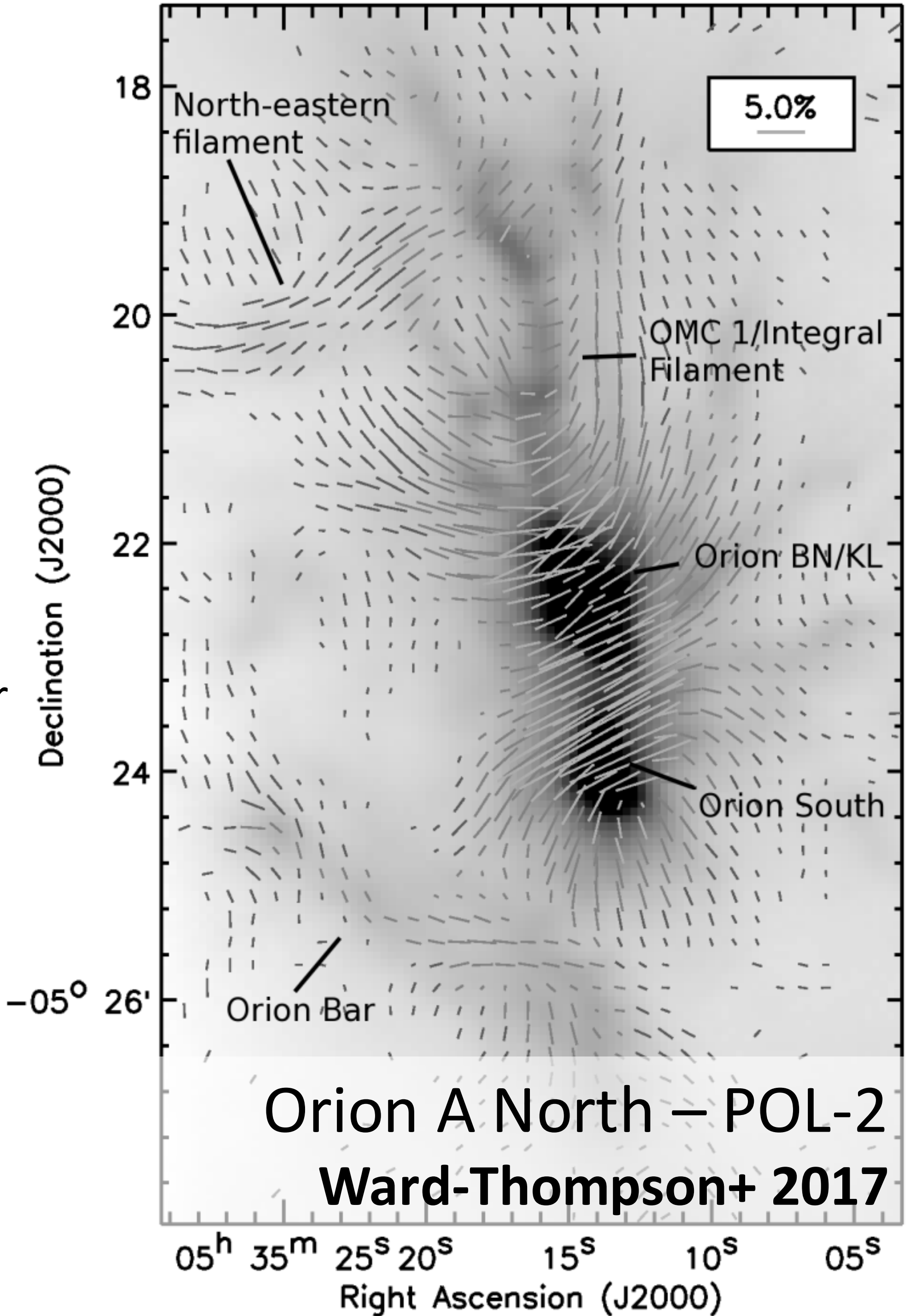

Stratospheric Observatory For Infrared Astronomy (SOFIA)

Flight Crew (i.e., Miracle Workers)

Elizabeth Ruth, SOFIA pilot
Credit: NASA

Inside SOFIA

Credit: NASA

Observing on SOFIA – HAWC+

Observing on SOFIA – GREAT

Credit: "The Sky at Night", British Broadcasting Corporation

SOFIA Flight Plans

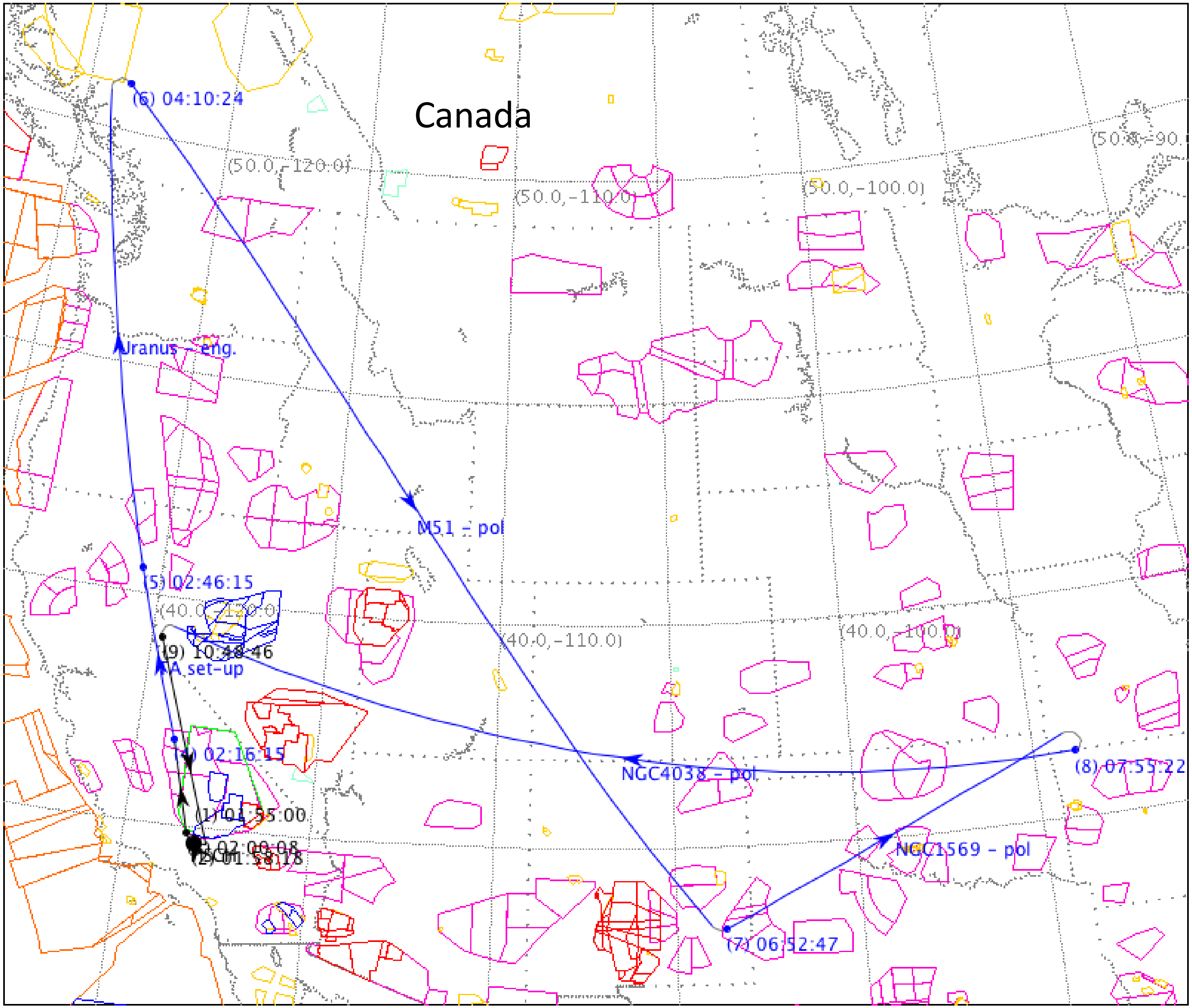

SOFIA Flight Plans

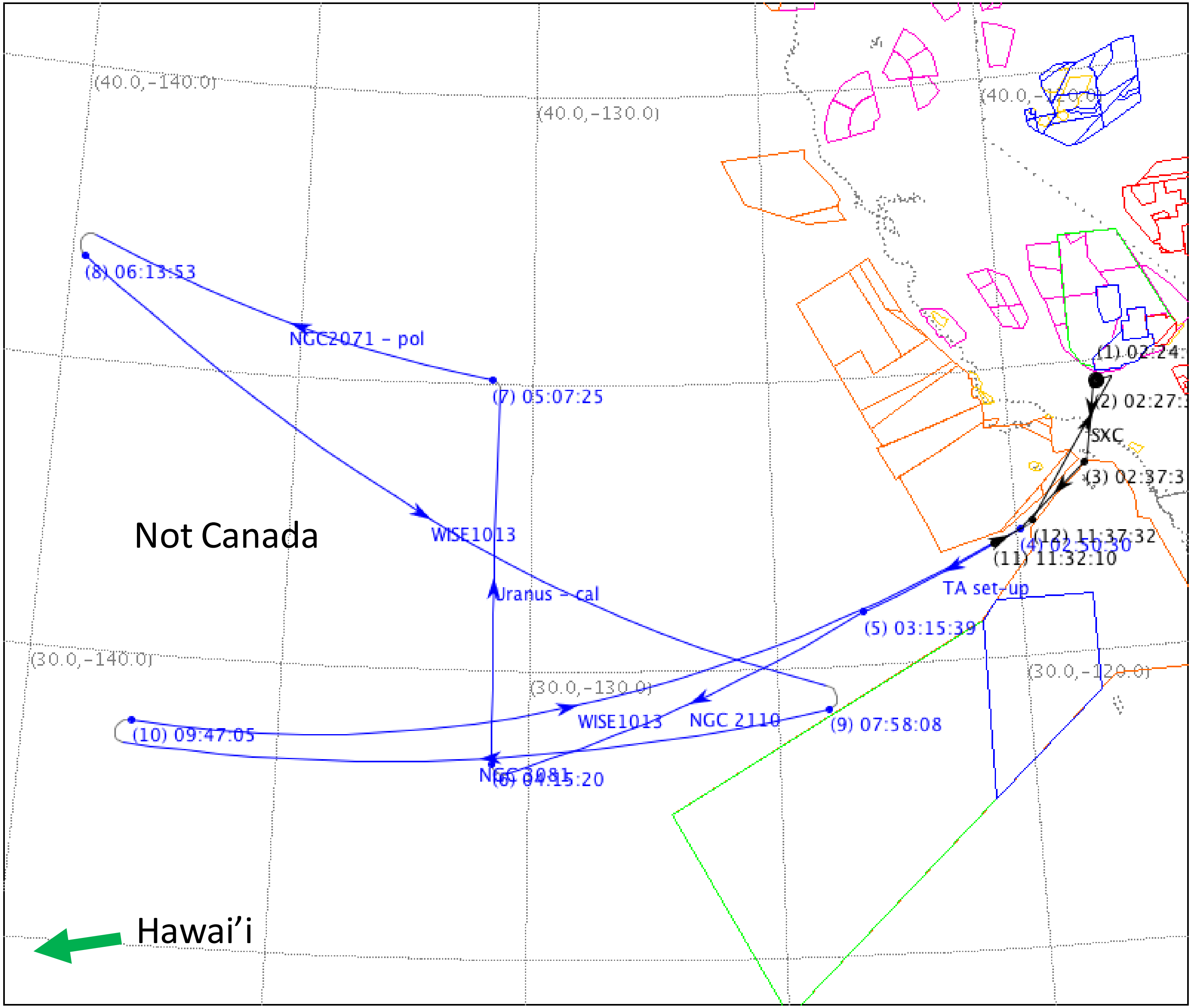

SOFIA Southern Deployment

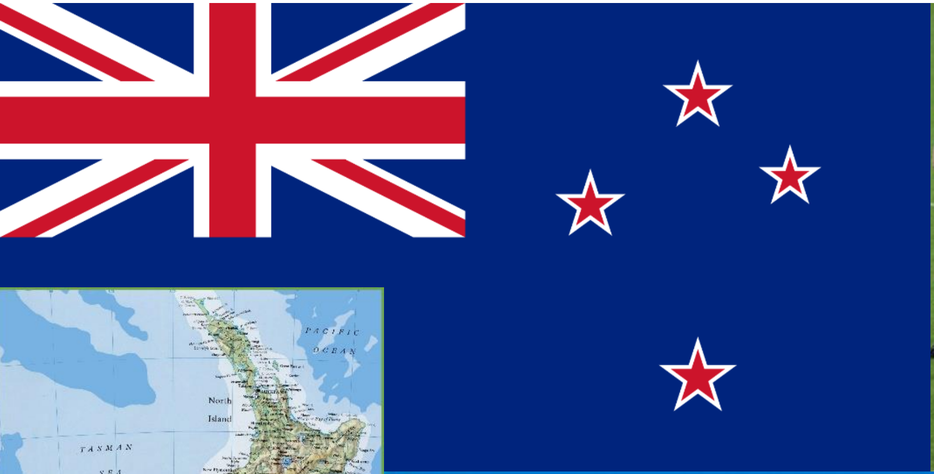

High-resolution Airborne Wide-band Camera (HAWC+)

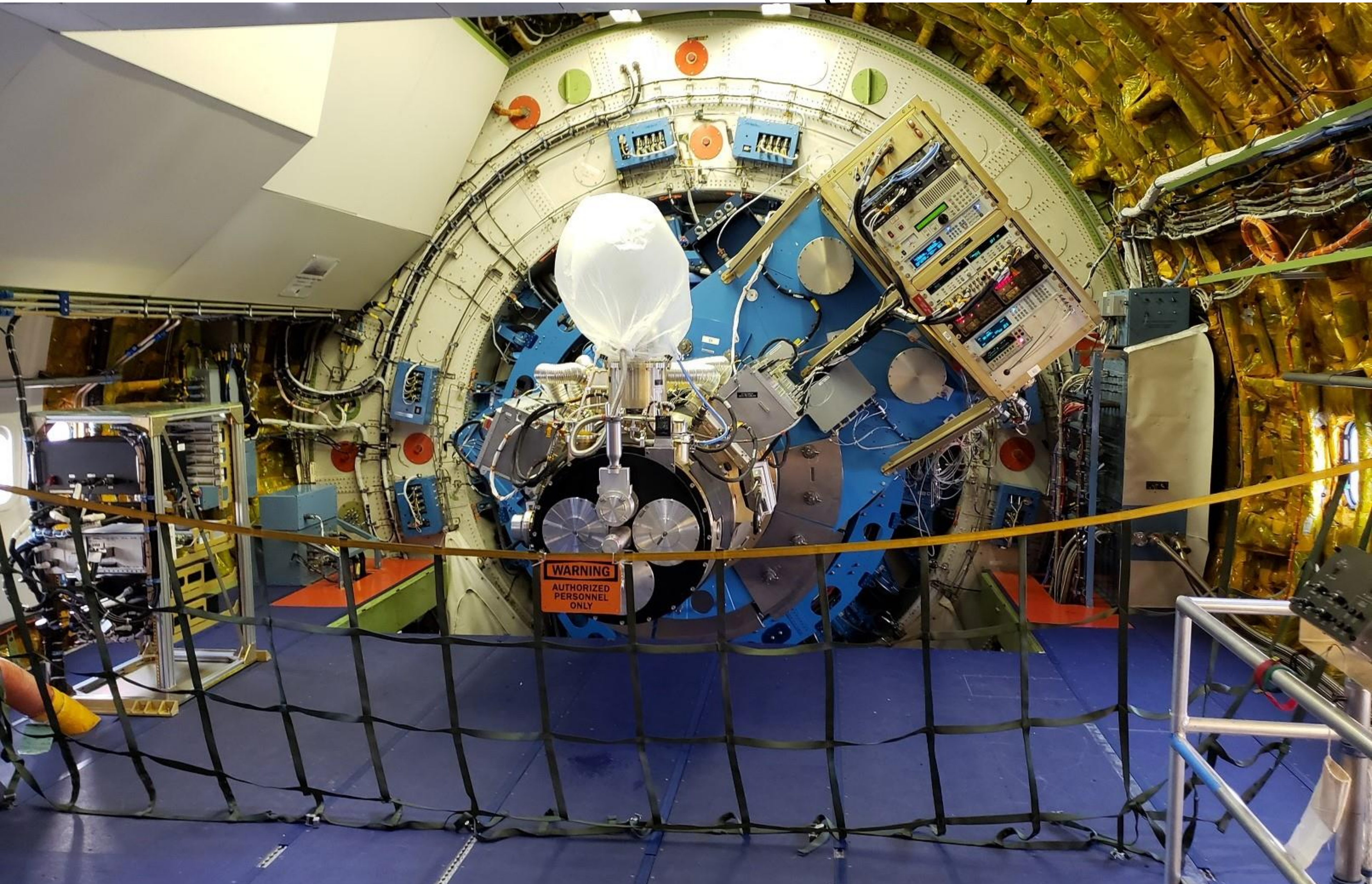

High-resolution Airborne Wide-band Camera (HAWC+)

Band / Wavelength	Δλ/λ	Angular Resolution	Total Intensity FOV (arcmin)	Polarization FOV (arcmin)
A / 53 µm	0.17	4.7" FWHM	2.7 x 1.7	1.3 x 1.7
B[a] / 63 µm	0.15	5.8" FWHM	4.2 x 2.6	2.1 x 2.6
C / 89 µm	0.19	7.8" FWHM	4.2 x 2.6	2.1 x 2.6
D / 154 µm	0.22	14" FWHM	7.3 x 4.5	3.6 x 4.5
E / 214µm	0.20	19" FWHM	8.0 x 6.1	4.0 x 6.1

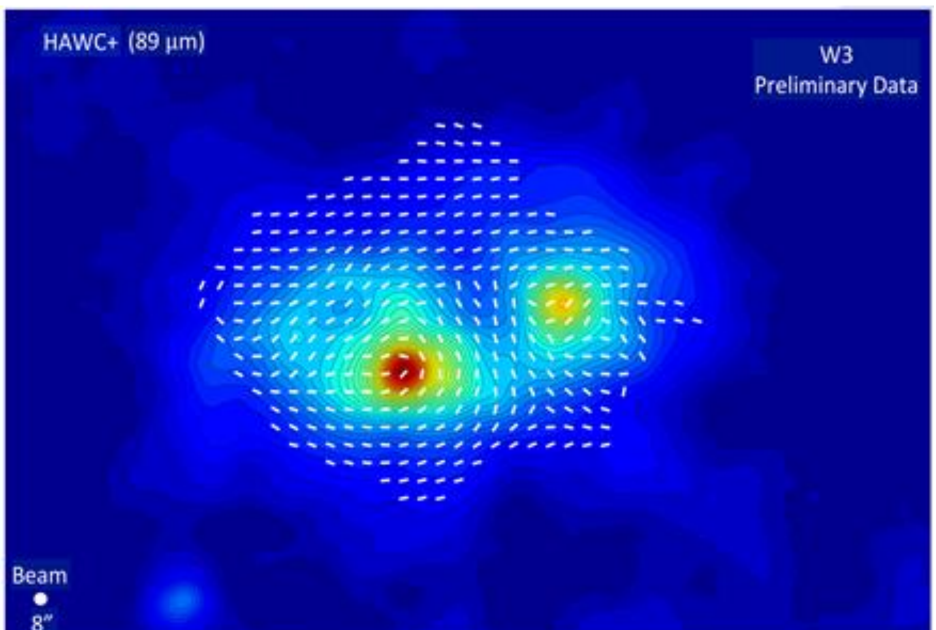

Above: Characteristics of the four HAWC+ bands. Polarization is obtained using a chop-nod observing mode
Harper+ 2018

Left: 89 µm polarization towards the W3 star-forming region

BLAST-TNG

Coming December ~~2018~~ 2019!

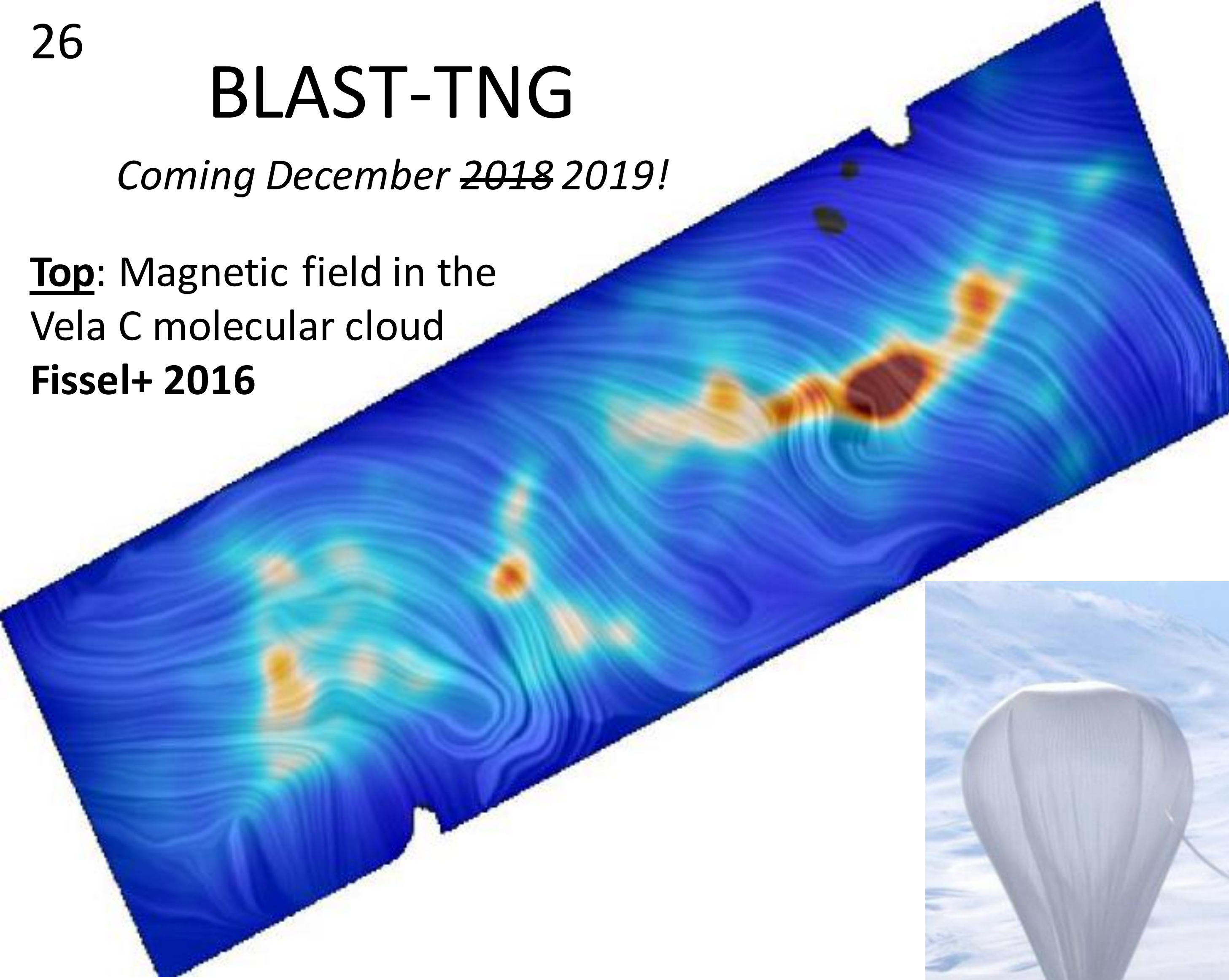

Top: Magnetic field in the Vela C molecular cloud
Fissel+ 2016

Bottom: BLAST-Pol in Antarctica
December 2010
Credit: BLAST team

Atacama Large Millimeter Array (ALMA)

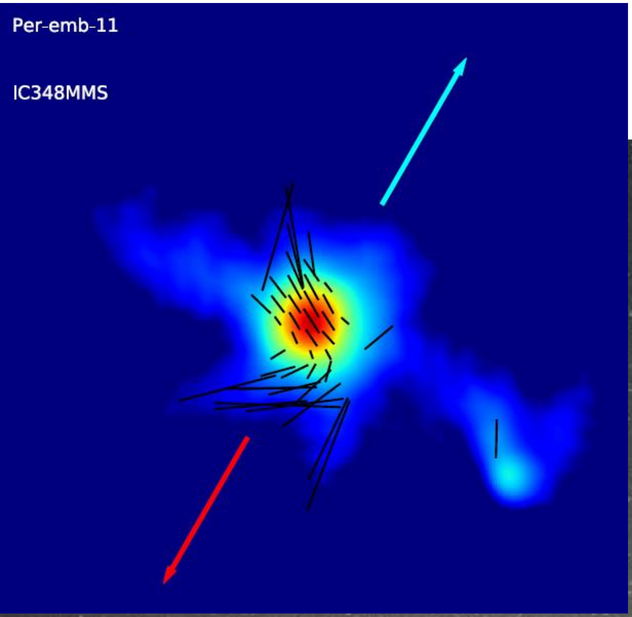

<u>Left</u>: 870 μm polarization towards a protostar in Perseus – **Cox+ 2018**

Don’t Forget Spectroscopy

Above: Ammonia observations of the Orion A with GAS – **Friesen+ 2018**

Left: Green Bank Telescope

3. Dynamics of Star-Forming Regions

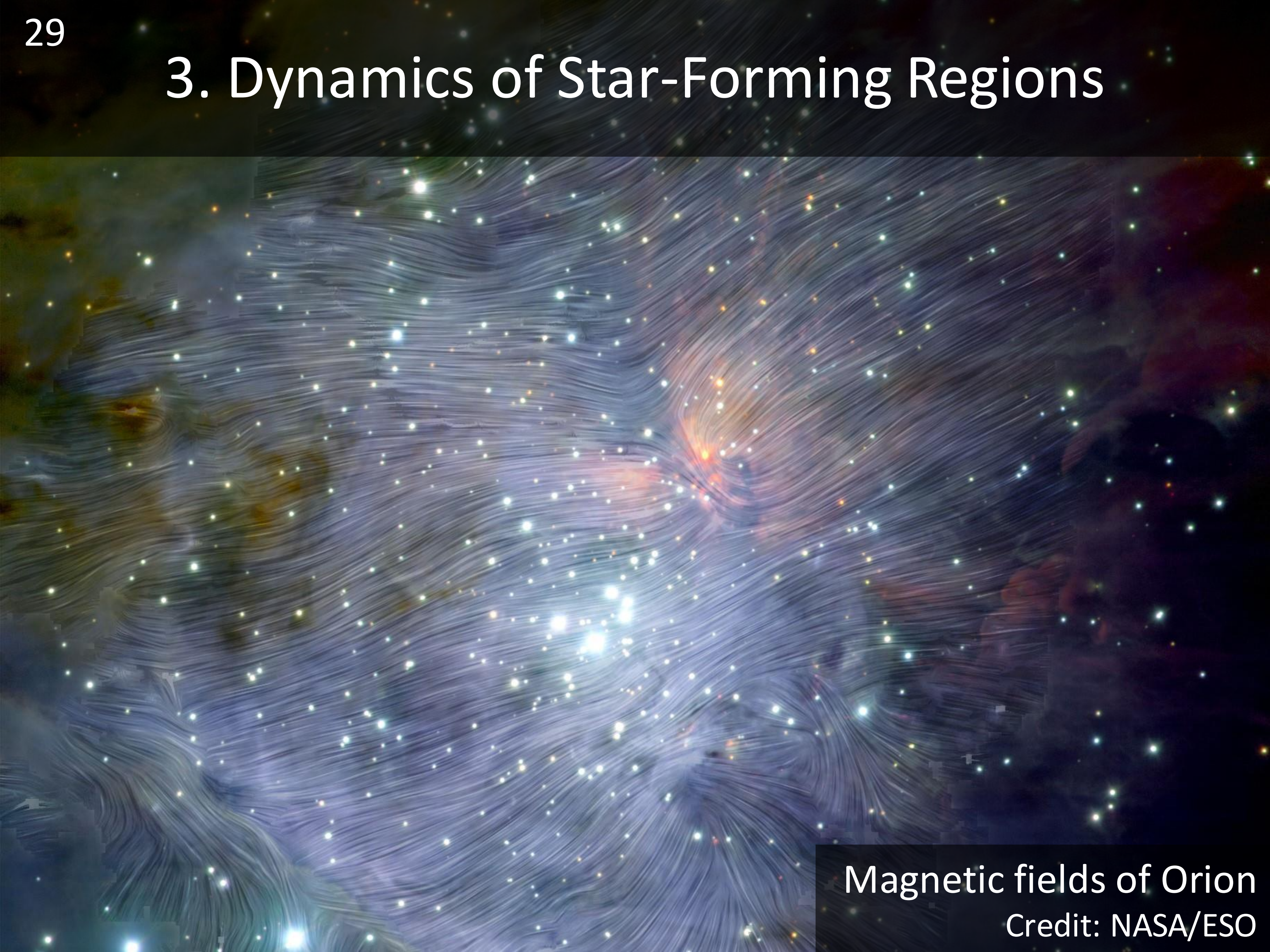

Magnetic fields of Orion
Credit: NASA/ESO

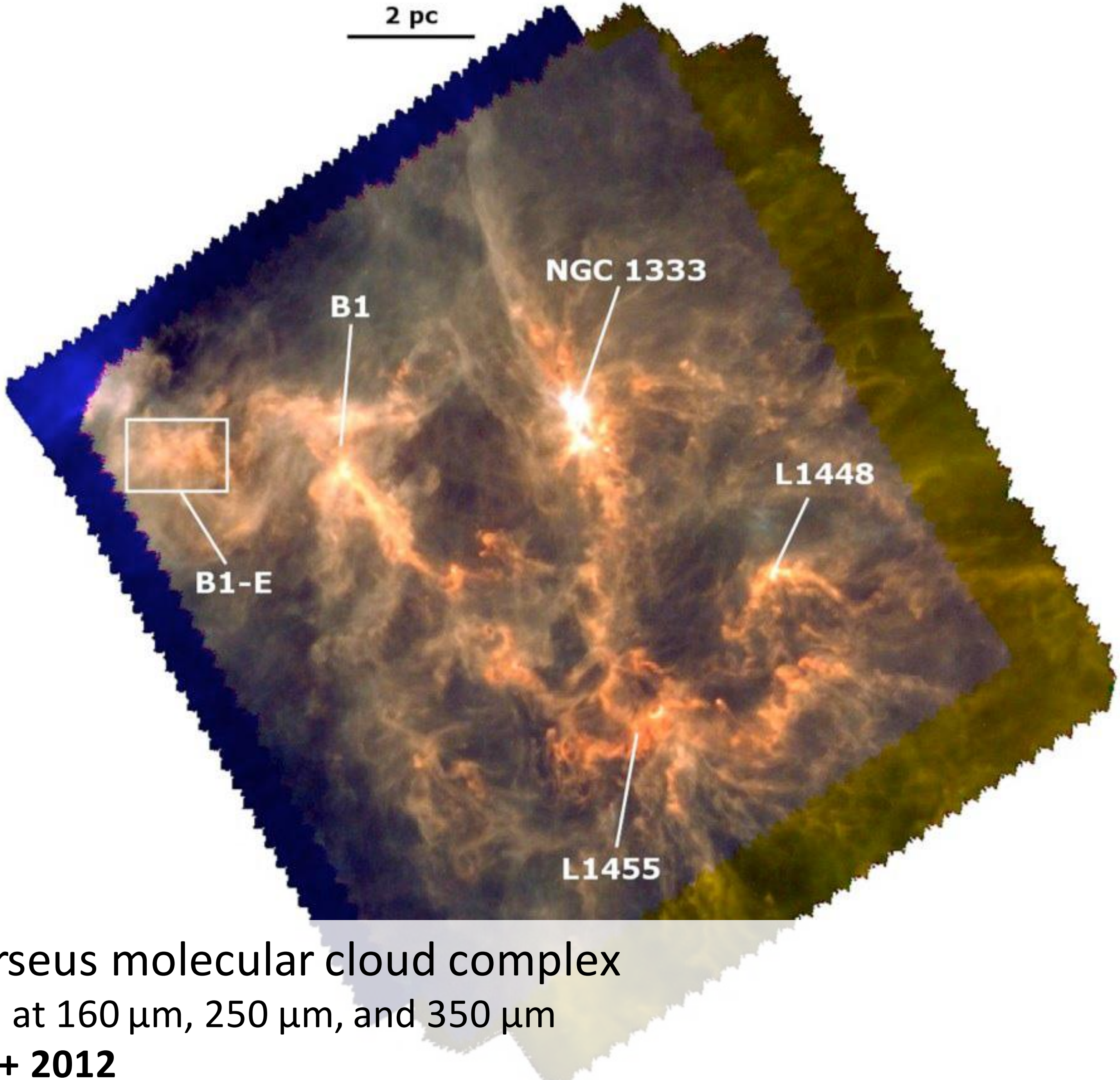

The Perseus molecular cloud complex

Herschel at 160 µm, 250 µm, and 350 µm

Sadavoy+ 2012

Magnetic Fields in Filaments and Cores

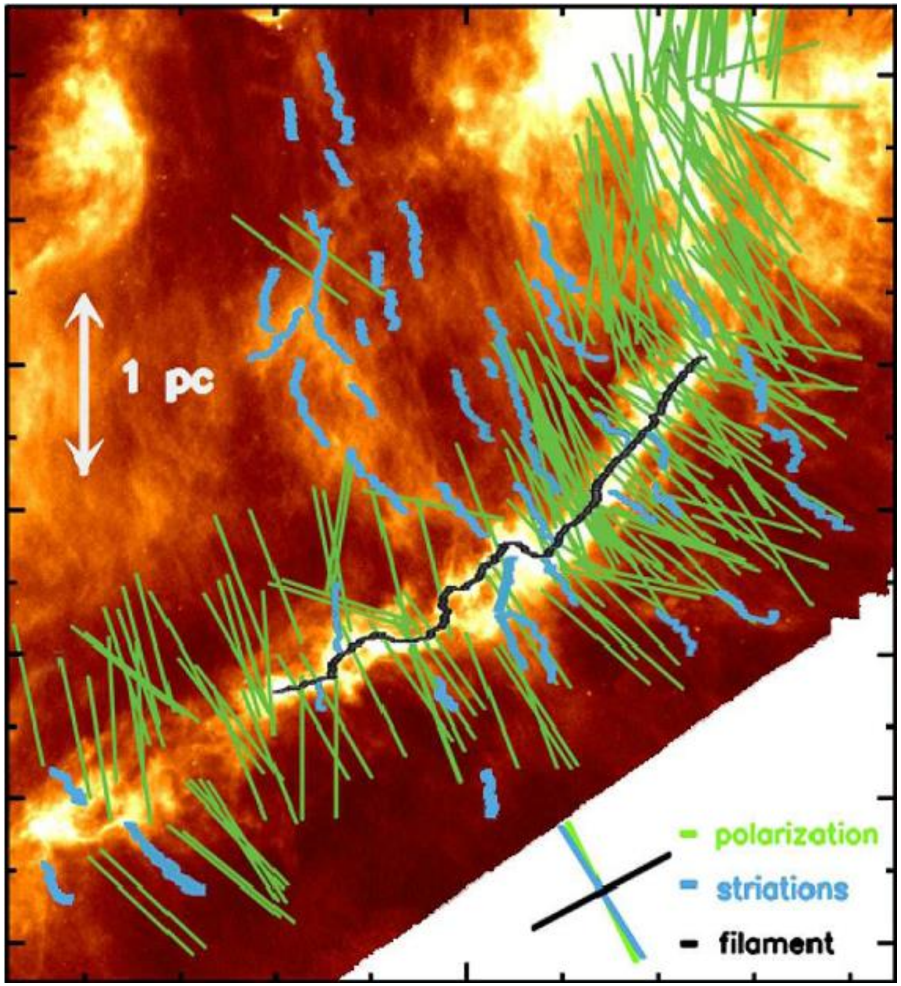

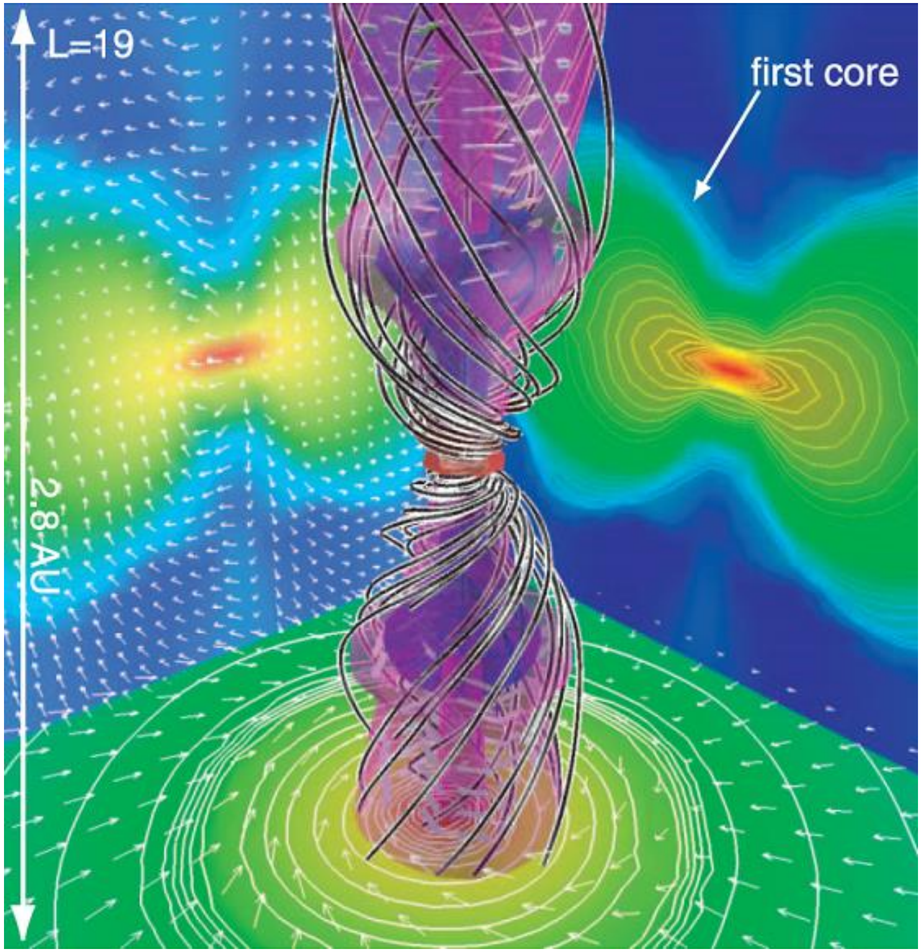

Left: Plane-of-sky magnetic field in Taurus relative to filaments and sub-filaments
André+ 2014

Right: Magnetohydrodynamic simulation of a protostellar outflow and jet
Machida, Inutsuka & Matsumoto 2008

Relation Between Outflows and Filaments

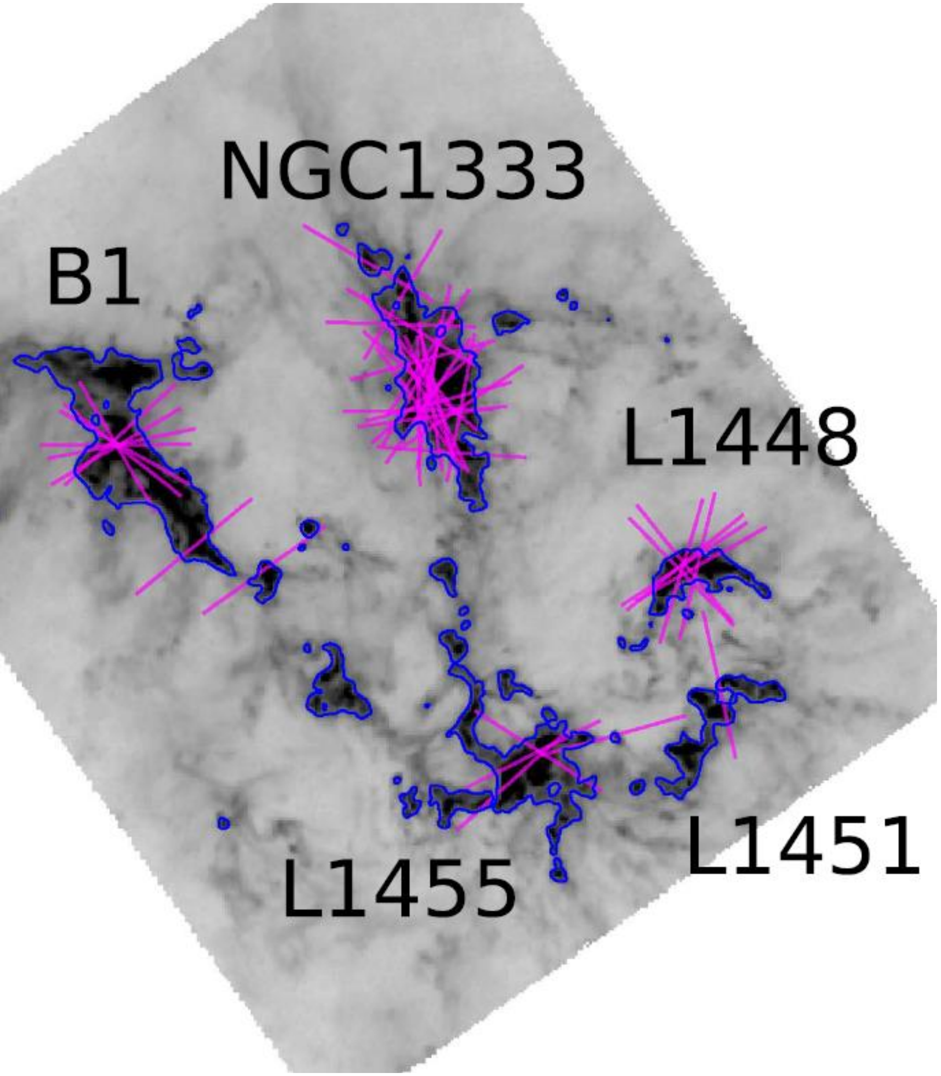

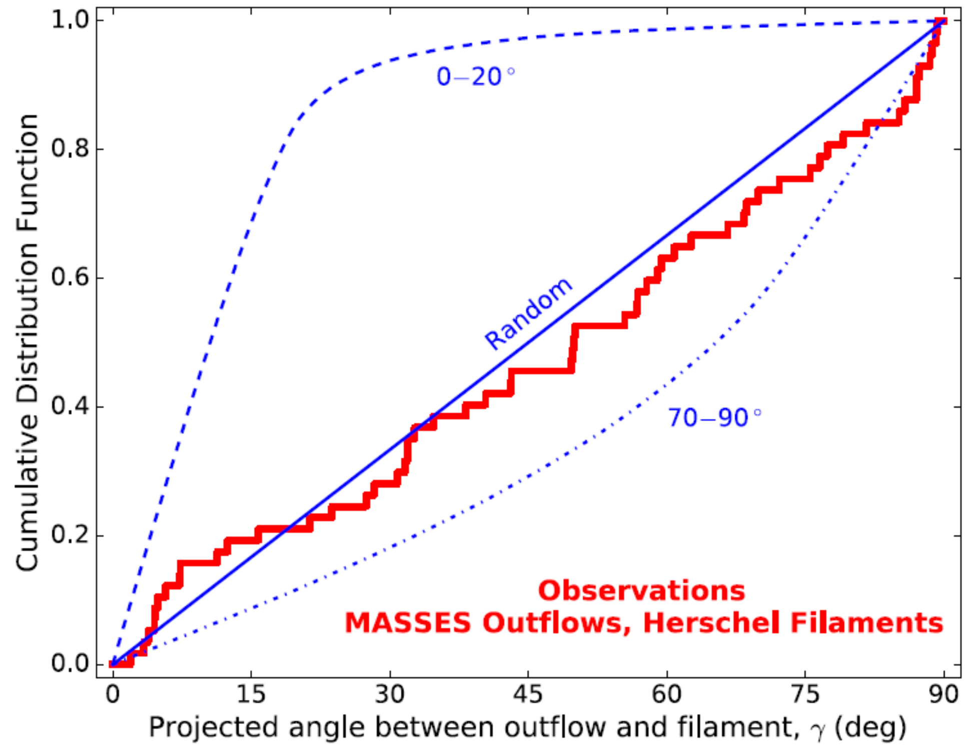

Left: Outflows in the Perseus complex
Stephens+ 2017

Right: Distribution of projected angles between outflows and filaments
Stephens+ 2017

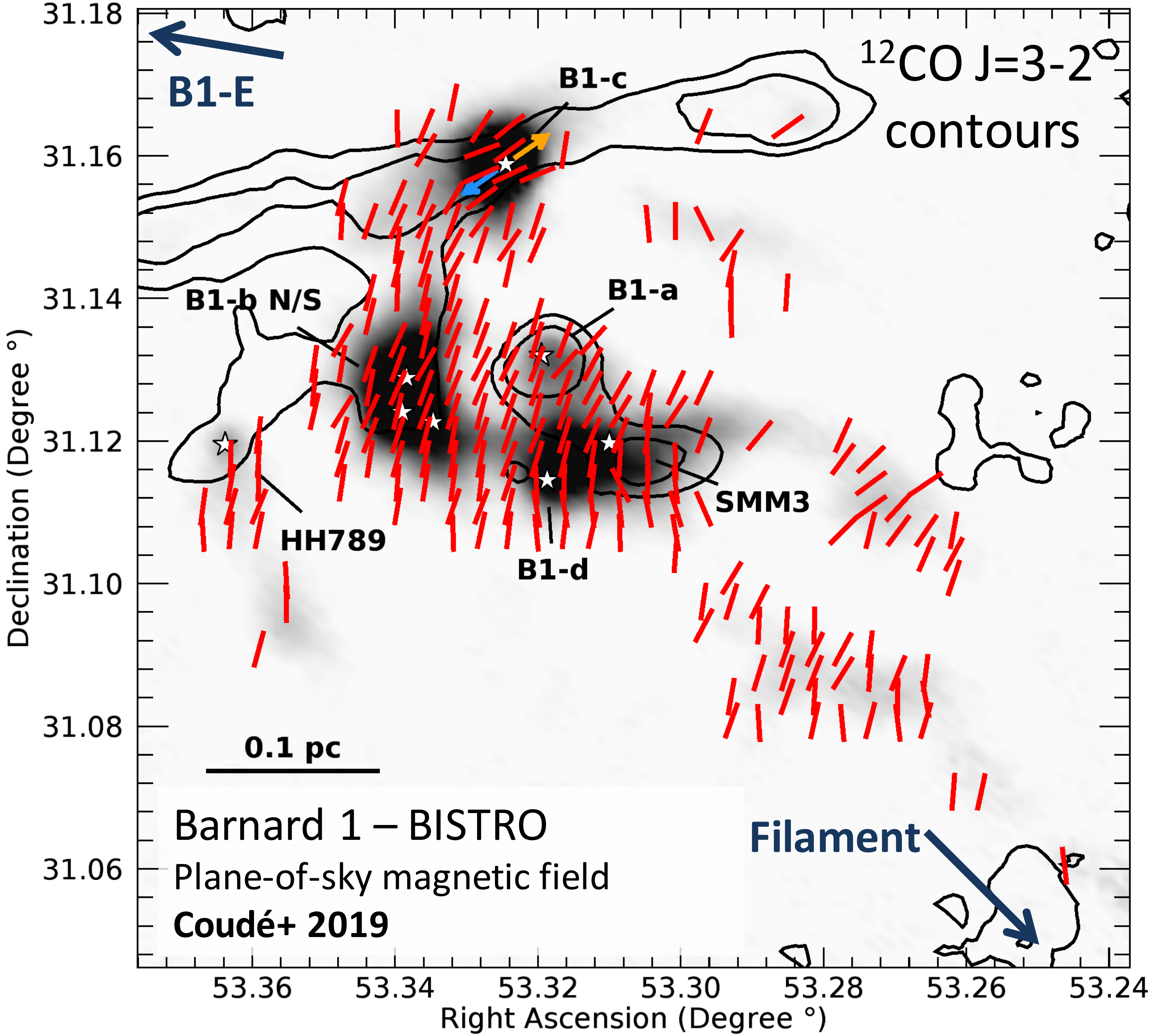

Barnard 1 – BISTRO

Plane-of-sky magnetic field

Coudé+ 2019

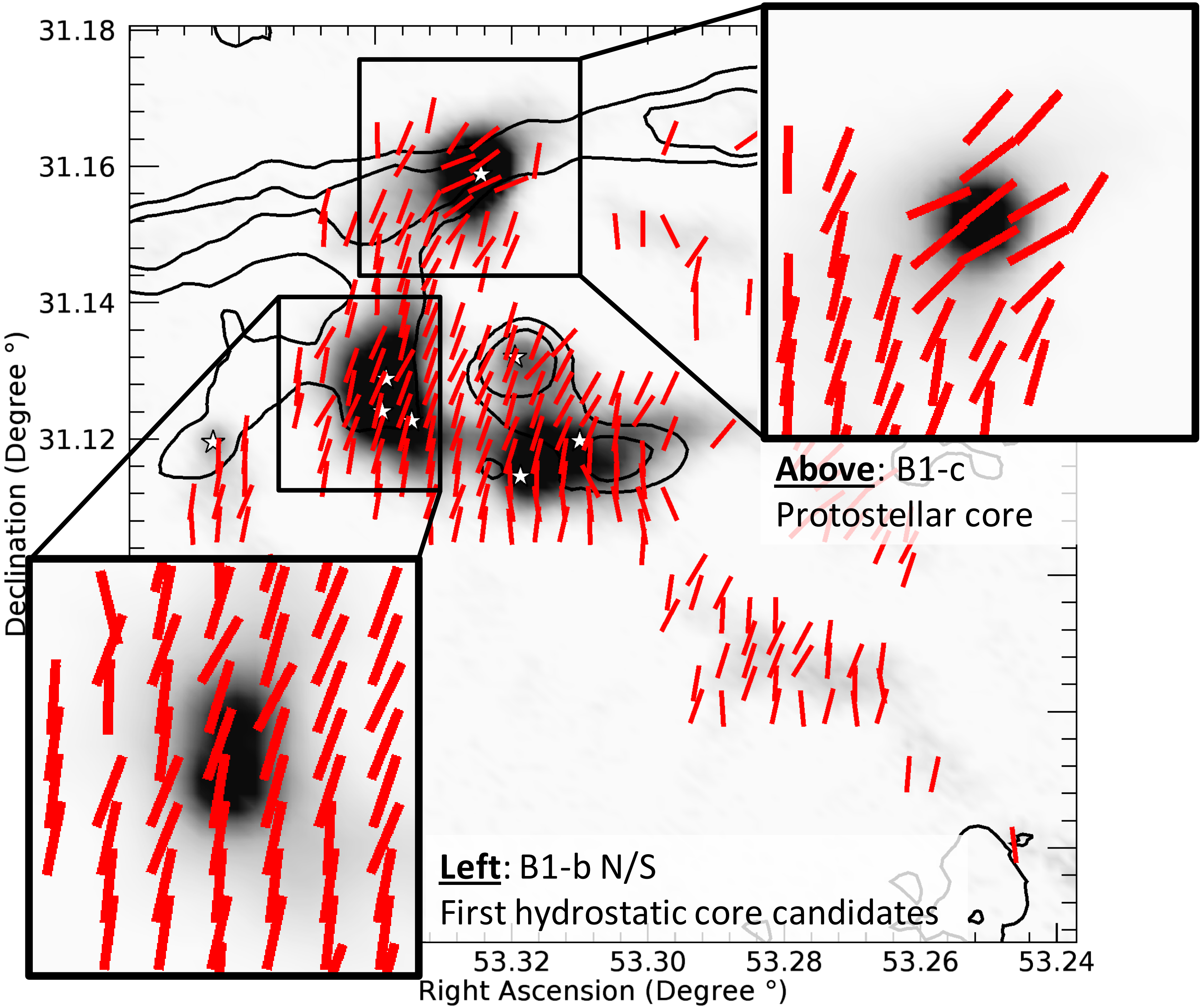
31.18
31.16
31.14
31.12
Declination (Degree °)
53.32
53.30
53.28
53.26
53.24
Right Ascension (Degree °)
Above: B1-c
Protostellar core
Left: B1-b N/S
First hydrostatic core candidates

Misalignment Between Magnetic Field and Angular Momentum in Protostellar Cores

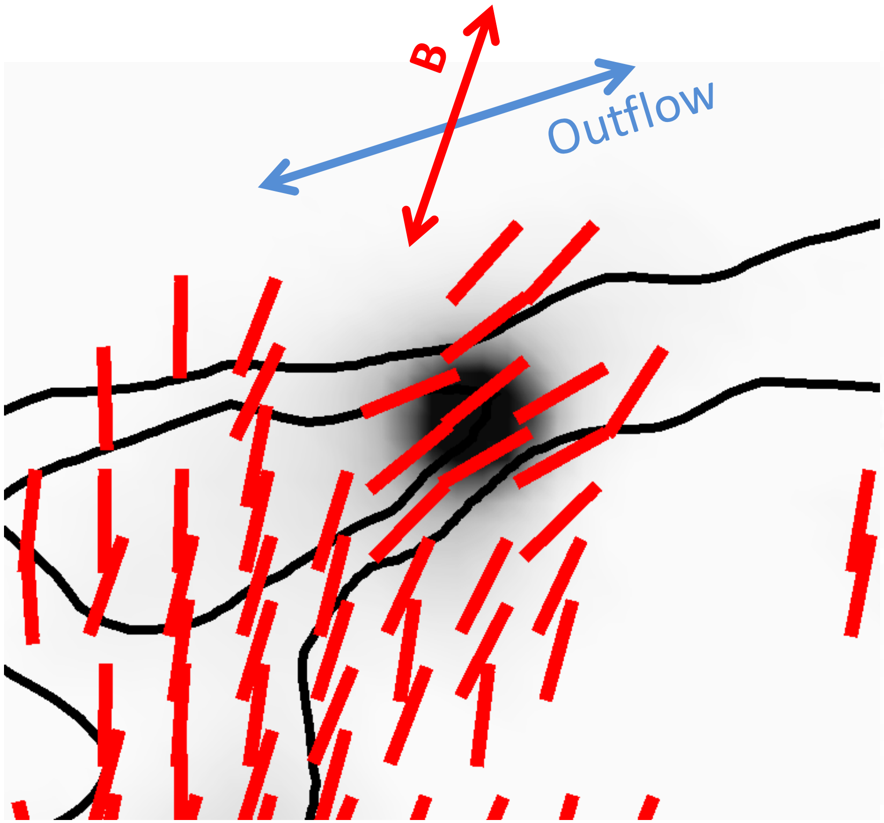

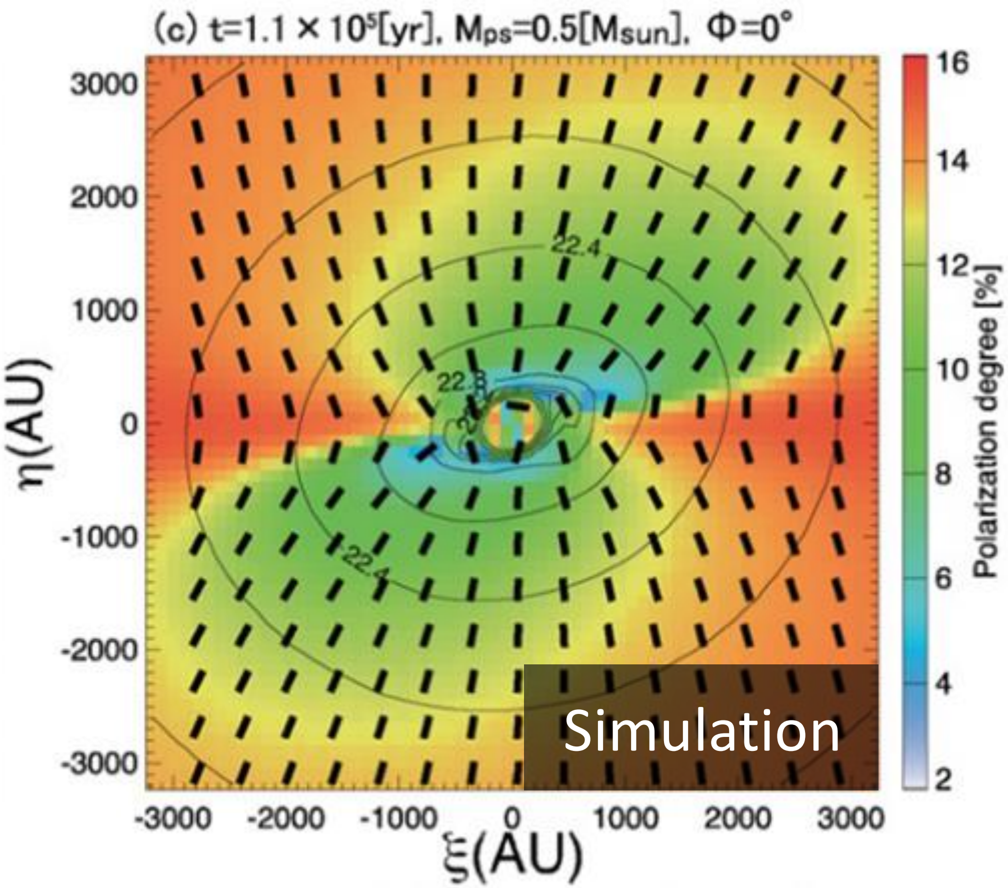

Left: Protostellar core B1-c
Plane-of-sky magnetic field and molecular outflow

Right: Misaligned protostellar core
Kataoka, Machida & Tomisaka 2012

Misalignment Between Magnetic Field and Angular Momentum in Protostellar Cores

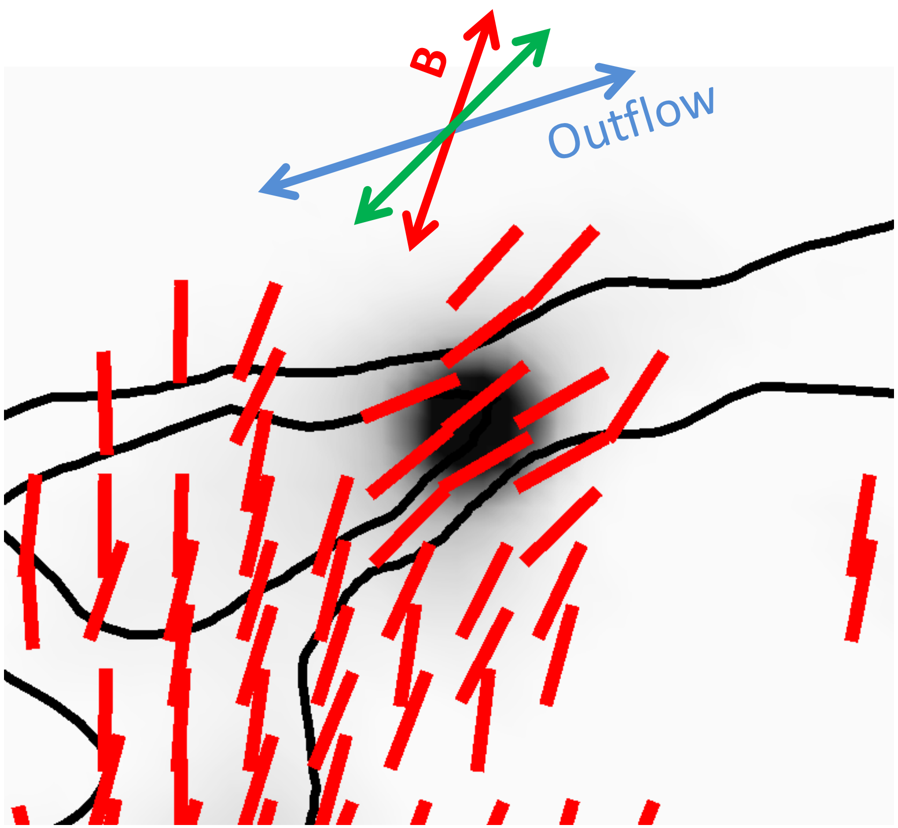

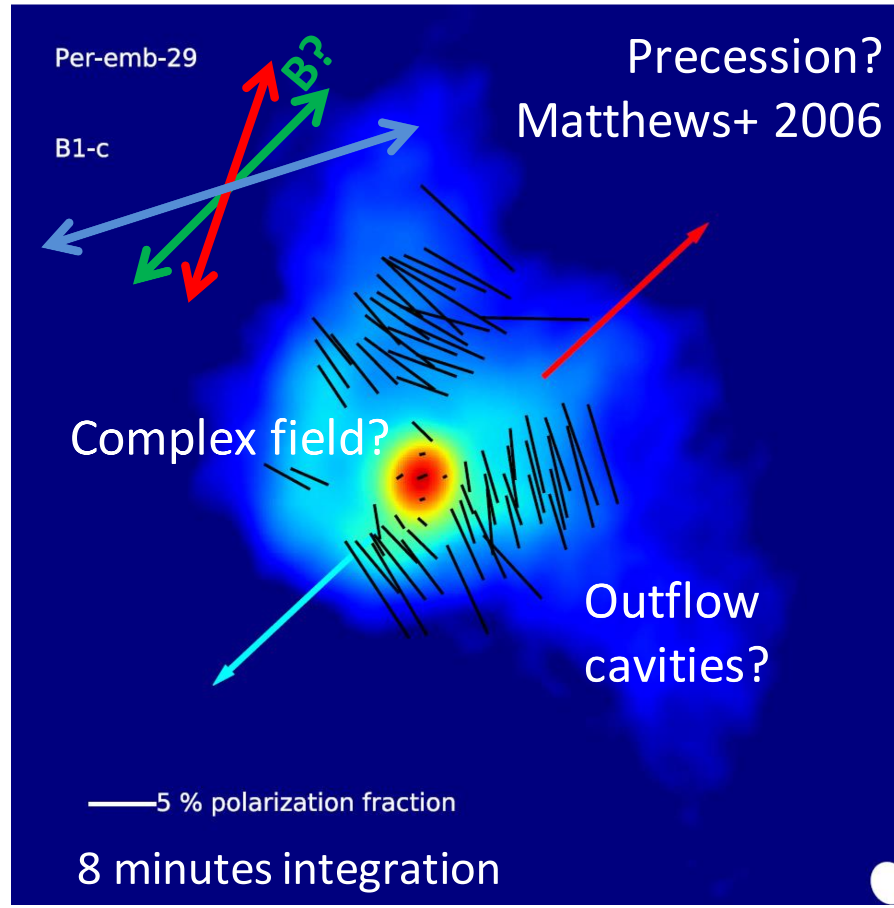

Left: Protostellar core B1-c
Plane-of-sky **magnetic field** and molecular outflow

Right: Protostellar core B1-c
Non-rotated ALMA **polarization** map
Cox+ 2018

Simulations of Magnetic Fields in Cores

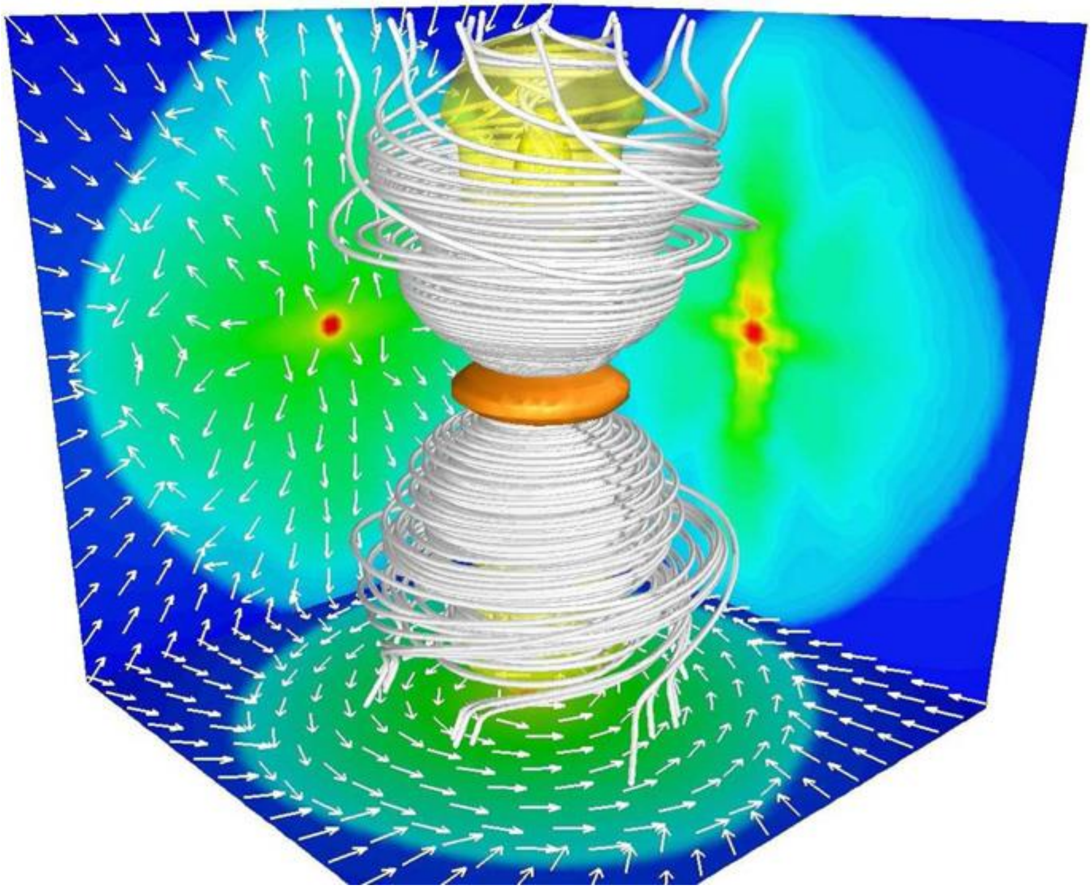

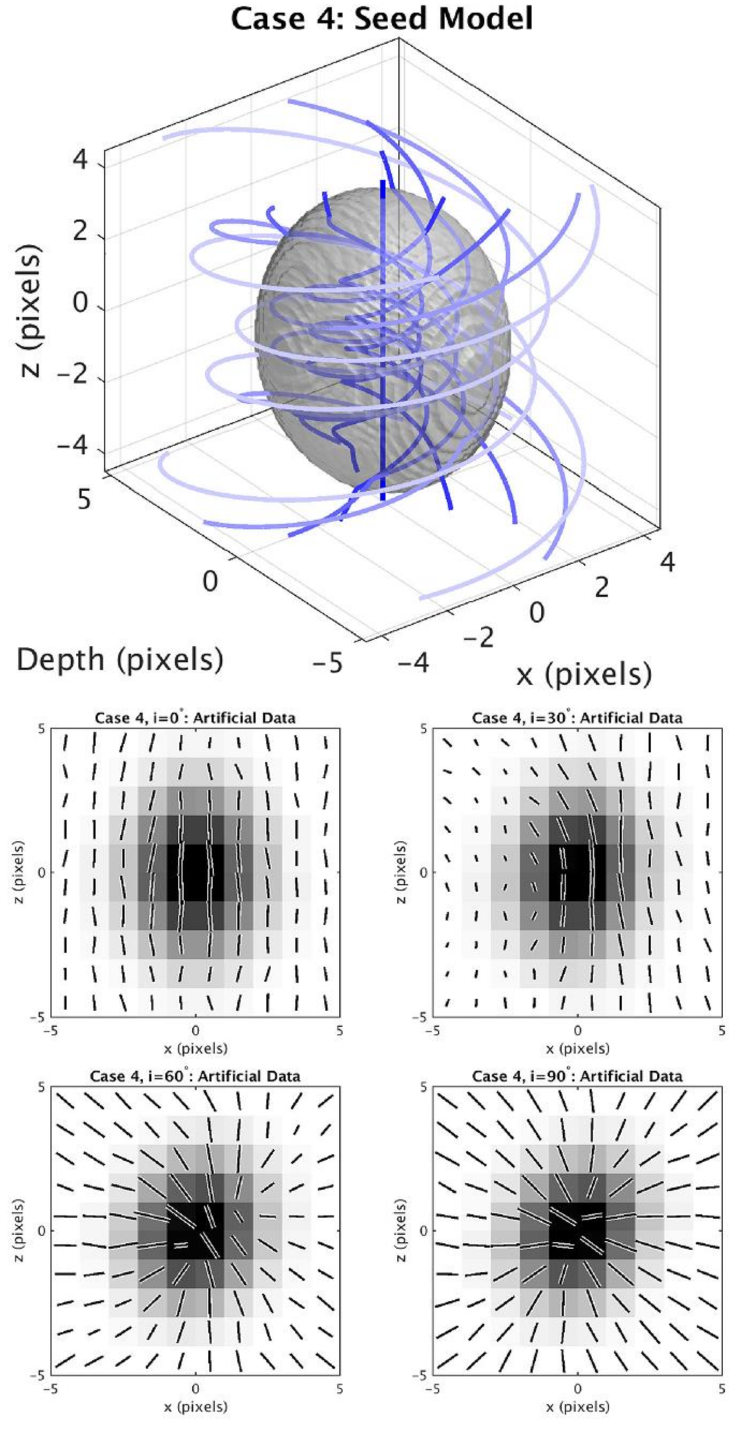

Left: Protostellar outflow model – **Tomida+ 2013**

Right: Polarisation model for a non-trivial magnetic field – **Franzmann & Fiege 2017**

Angular Dispersion Function – **Houde+ 2009**

$$f(\Delta\Phi) \approx \frac{1}{N}\frac{\langle B_t^2\rangle}{\langle B_o^2\rangle} - b^2(l) + al^2$$

Angular Dispersion Function

- $\langle \boldsymbol{B_t^2}\rangle / \langle \boldsymbol{B_o^2}\rangle$ – turbulent-to-ordered magnetic energy ratio
- $\boldsymbol{a}$ – first order Taylor coefficient

$$N \approx \Delta' \frac{(\delta^2 + 2W^2)}{\sqrt{2\pi}\,\delta^3}$$

Number of turbulent cells

- Δ' – effective cloud depth
- W – telescope beam width
- $\boldsymbol{\delta}$ – turbulent correlation length

$$b^2(l) = \frac{1}{N}\frac{\langle B_t^2\rangle}{\langle B_o^2\rangle} e^{-l^2/2(\delta^2+2W^2)}$$

Autocorrelation function

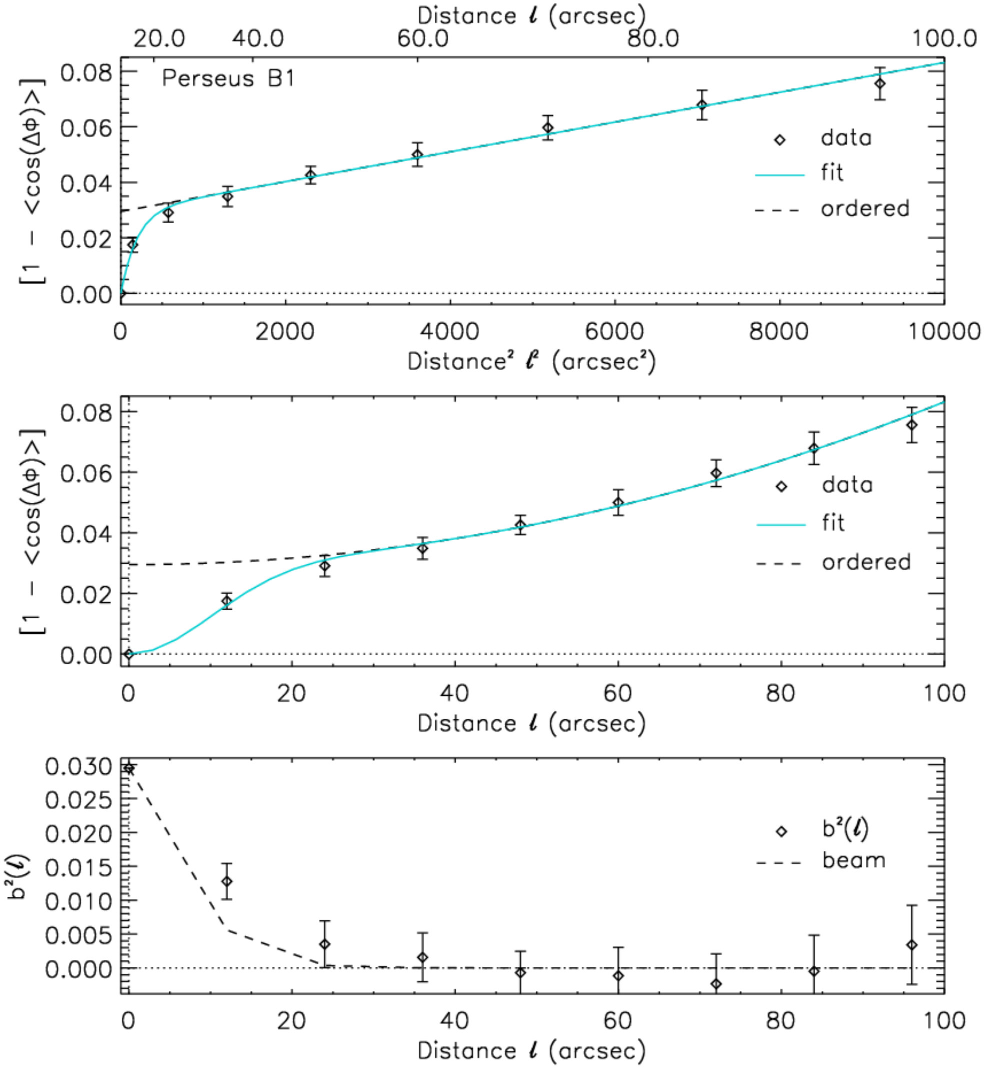

__**Right**__: Angular Dispersion Function for Barnard 1 – **Coudé+ 2019**

Amplitude of the Magnetic Field in Barnard 1

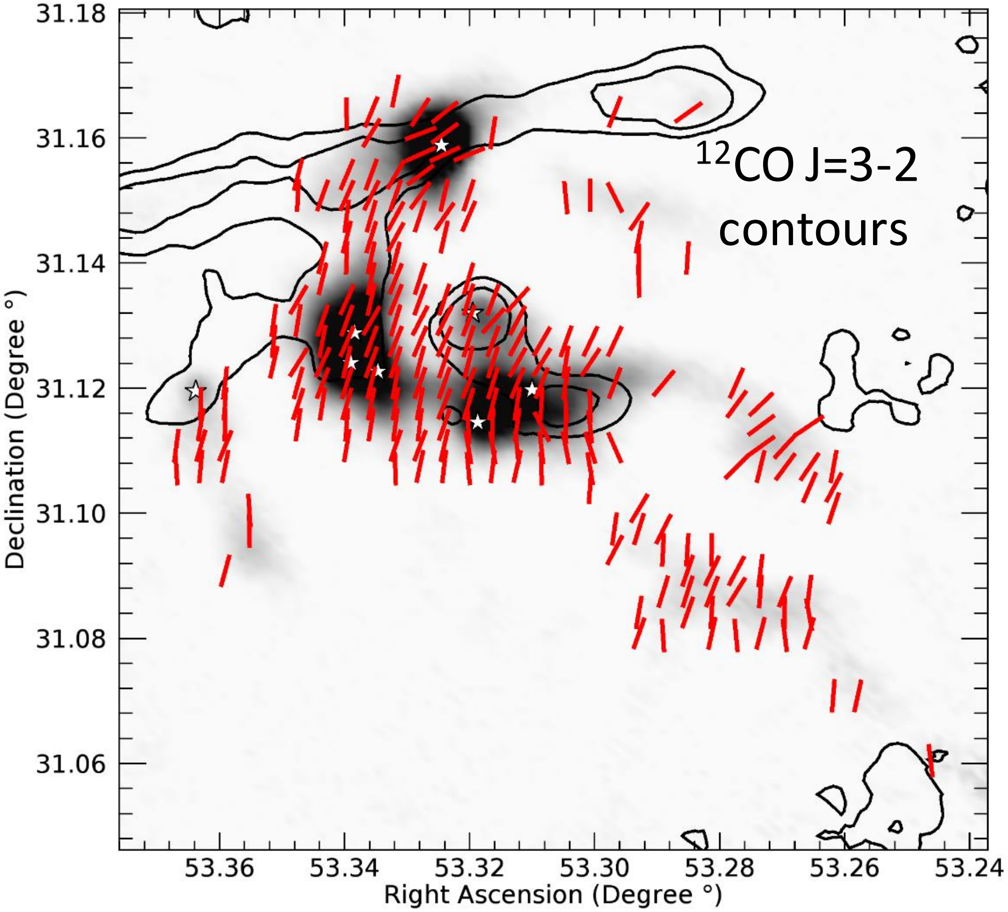

Left: Perseus B1 - BISTRO
Plane-of-sky magnetic field

$$B_{pos} \approx \sqrt{4\pi\rho}\ \delta V \left[\frac{\langle B_t^2\rangle}{\langle B^2\rangle}\right]^{-\frac{1}{2}}$$

Modified DCF equation

- δV – Velocity dispersion of the gas
  - NH_3 (1,1) – **GAS survey**
- ρ – Density of the gas
  - $n(H_2) = (1.5 \pm 0.3) \times 10^3$ cm^{-3}
  - **Friesen+ 2017, GAS+ in prep.**

Total magnetic energy ratio
$\langle B_t^2\rangle / \langle B^2\rangle = 0.5 \pm 0.3$

Turbulence correlation length
$\delta = 5.0'' \pm 2.5''$ *or 1500 au*

Magnetic field amplitude
$$\boldsymbol{B_{pos} \sim 120 \pm 60\ \mu G}$$

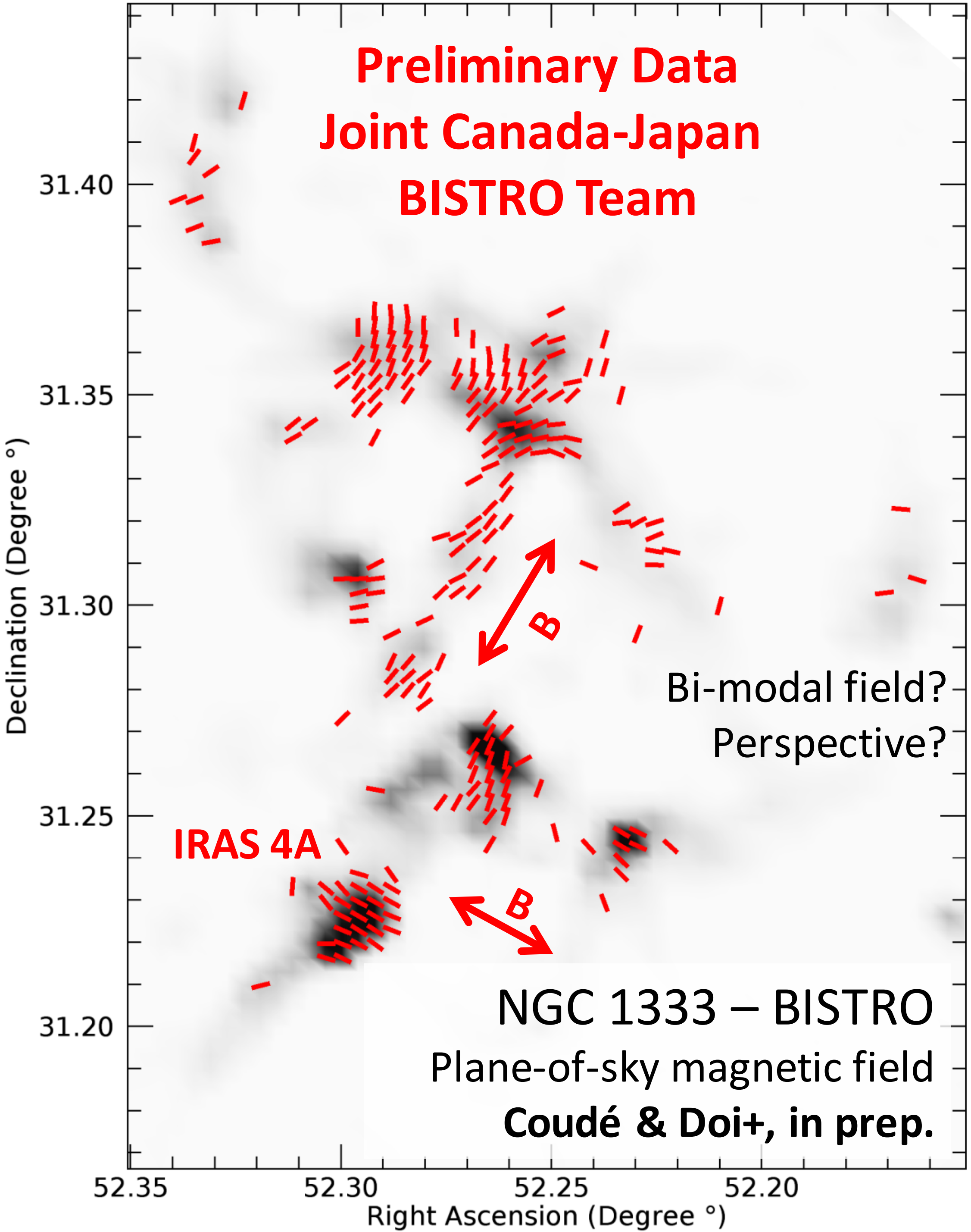
Preliminary Data
Joint Canada-Japan
BISTRO Team
31.40
31.35
31.30
31.25
31.20
Declination (Degree °)
B
Bi-modal field?
Perspective?
IRAS 4A
B
NGC 1333 – BISTRO
Plane-of-sky magnetic field
Coudé & Doi+, in prep.
52.35
52.30
52.25
52.20
Right Ascension (Degree °)

Magnetic Field in IRAS 4A

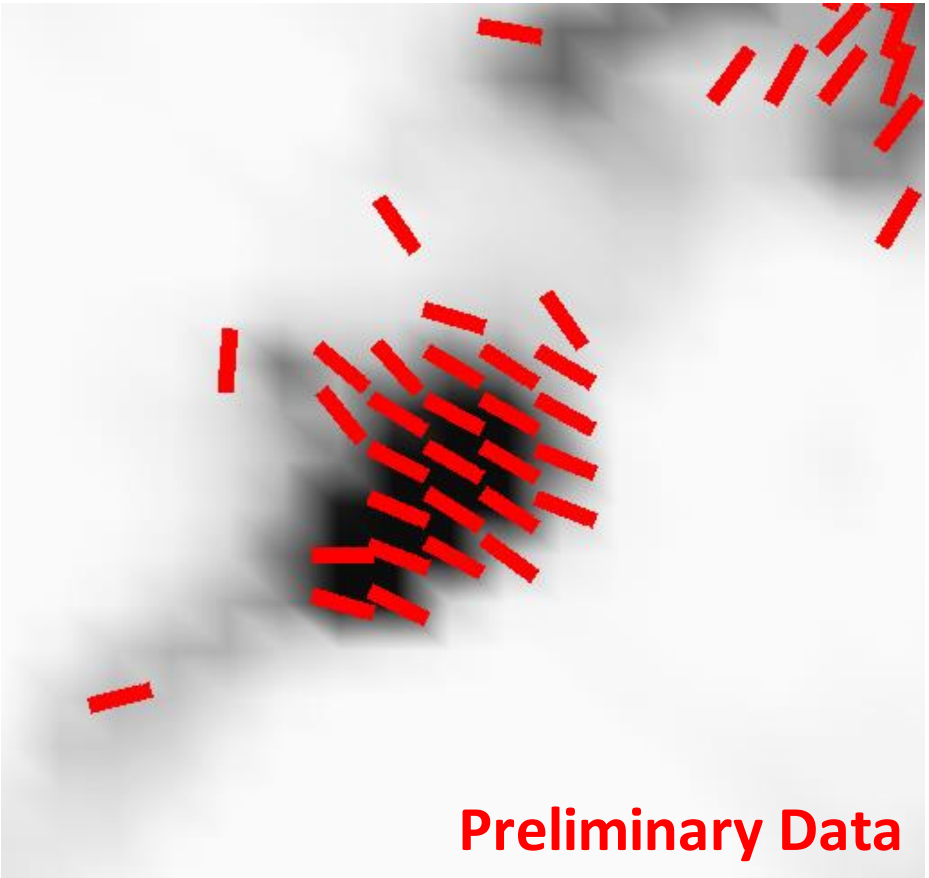

Left: IRAS 4A – BISTRO
Plane-of-sky magnetic field
Coudé & Doi+, in prep.

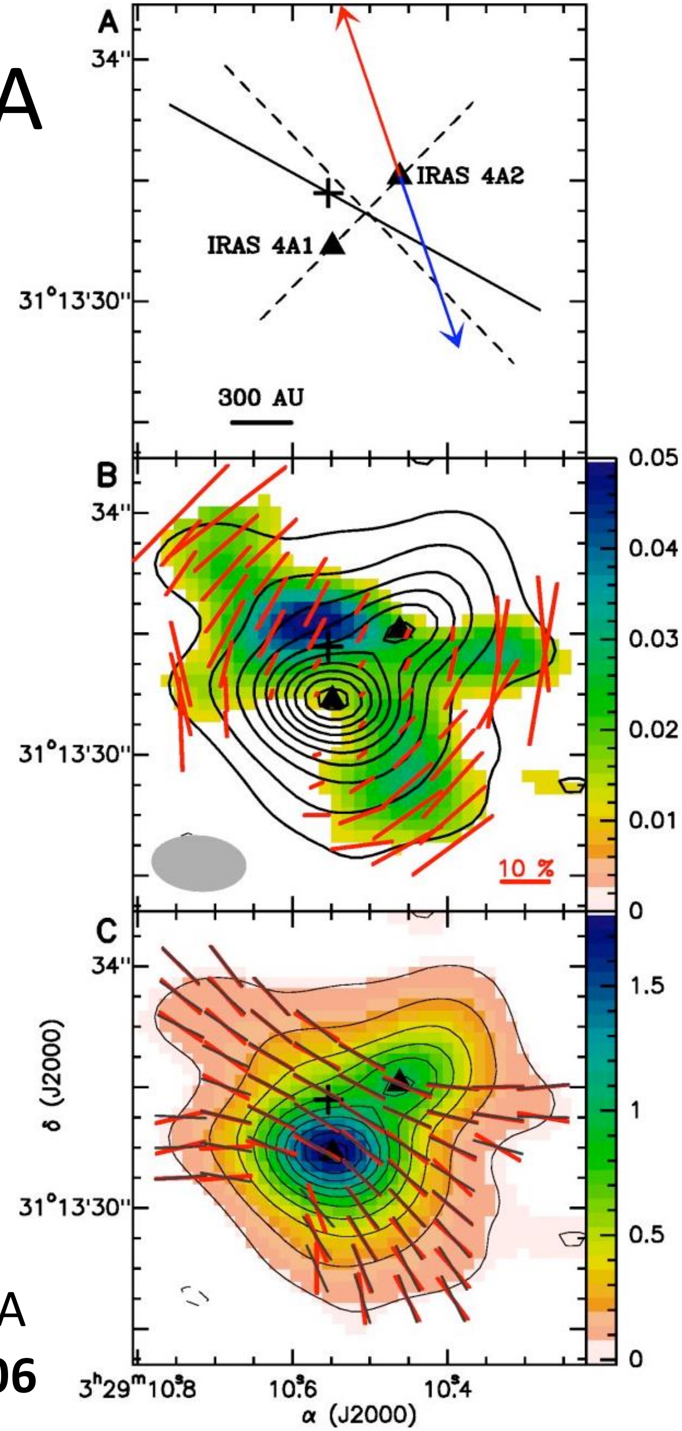

Right: SMA data of IRAS 4A
Girart, Rao & Marrone 2006

Magnetic Fields in Star-Forming Regions

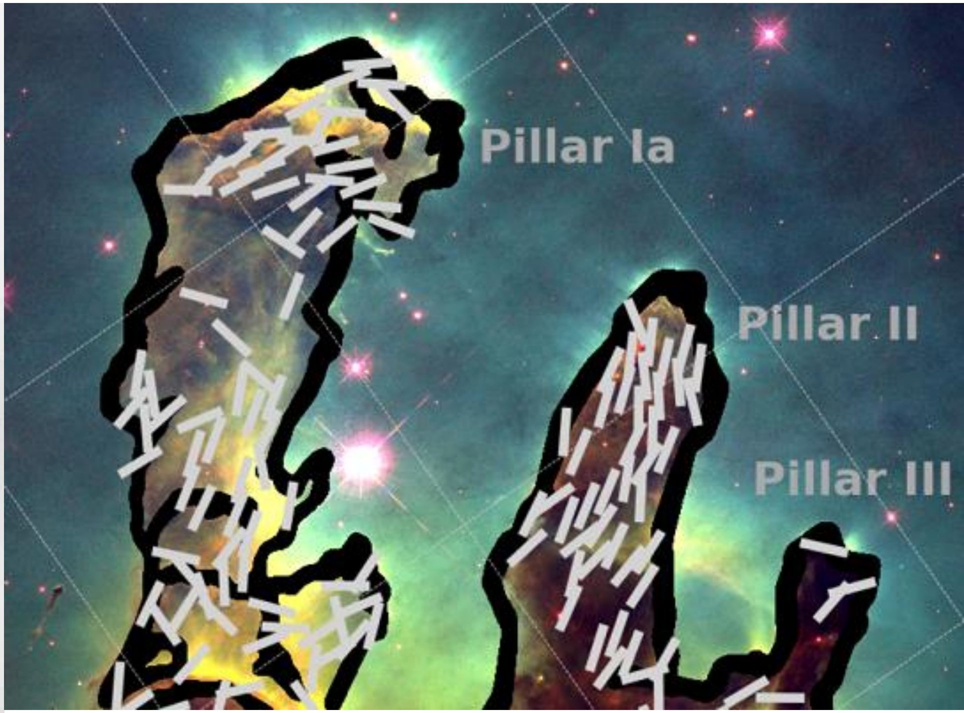

Above: Magnetic field in Messier 16. The magnetic field lines follow the length of the pillars.
Pattle+ 2018

Left: Magnetic field around the BN-KL outflow in Orion A.
Pattle+ 2017

Magnetic Fields in Star-Forming Regions

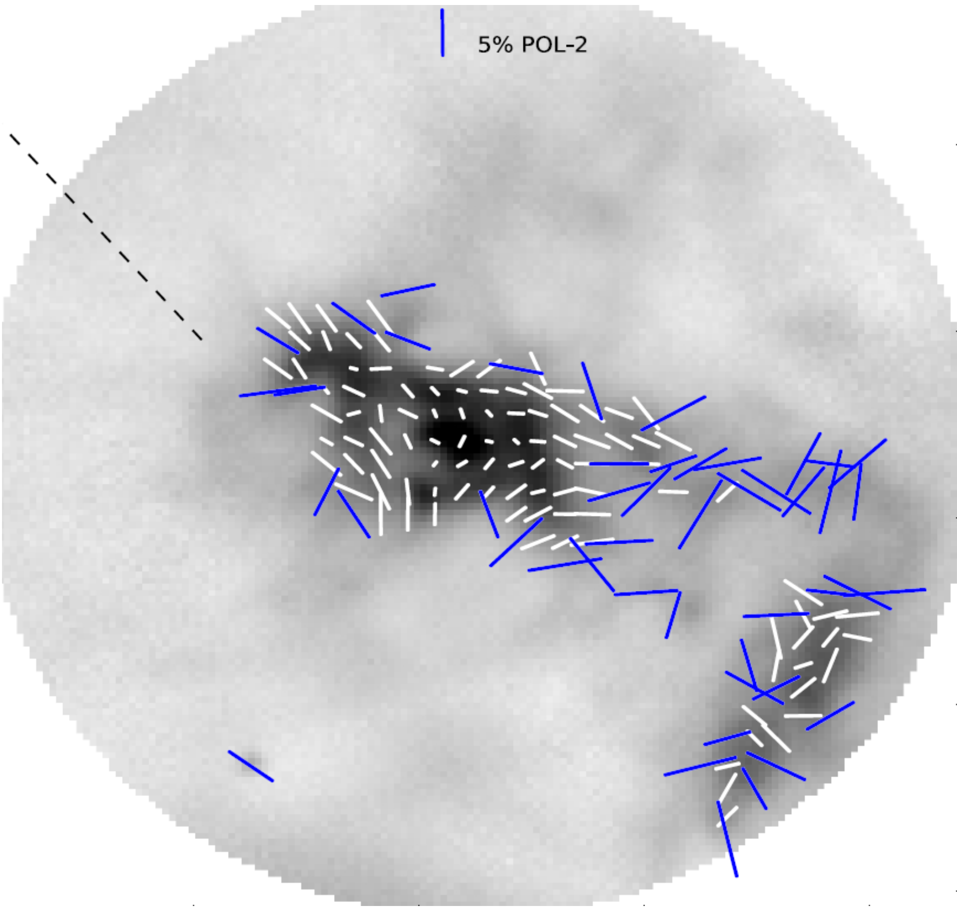

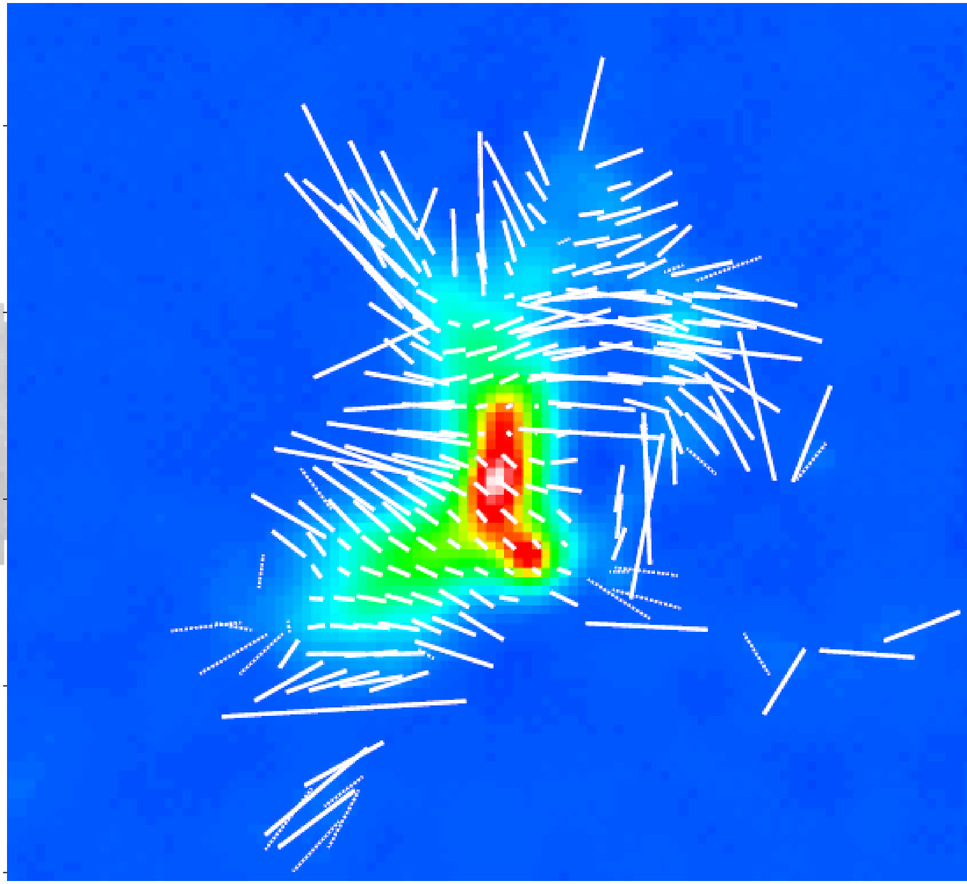

Left: Magnetic field orientation in the ρ Ophiuchus B clump.
Soam+ 2018

Right: Magnetic field orientation in the ρ Ophiuchus A clump.
Kwon+ 2018

Magnetic Fields in Star-Forming Regions

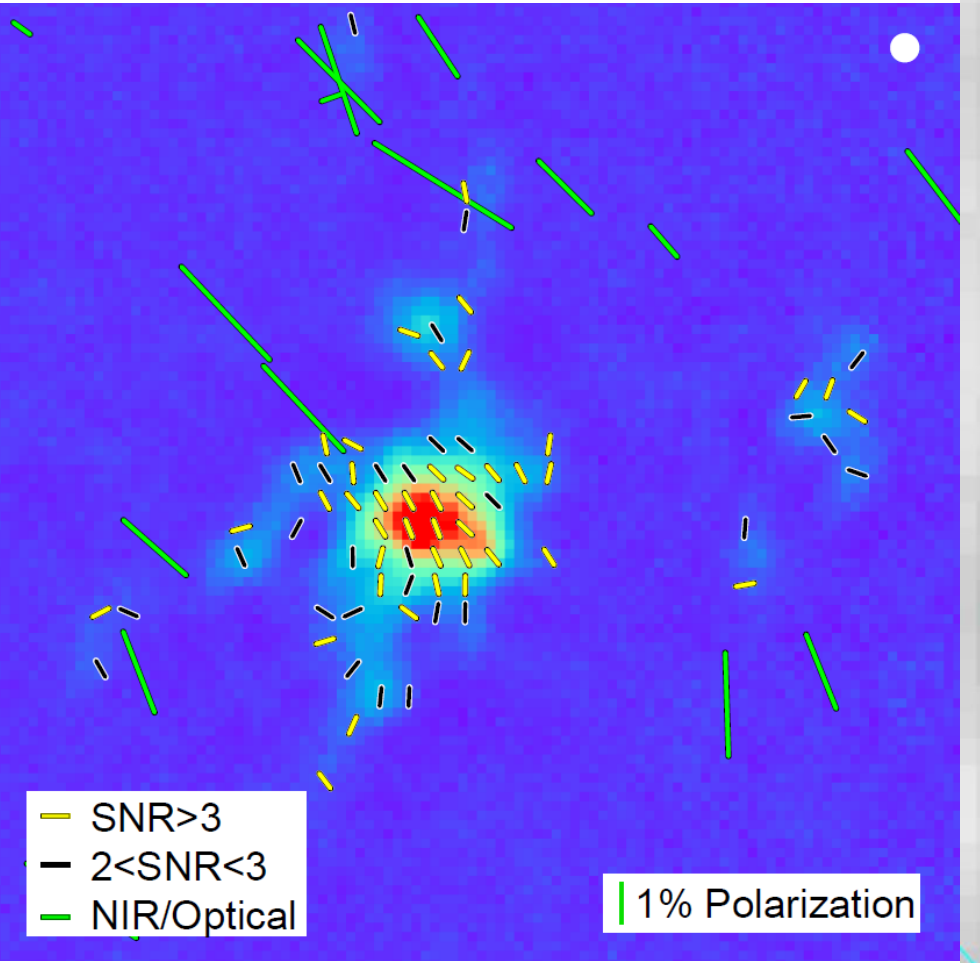

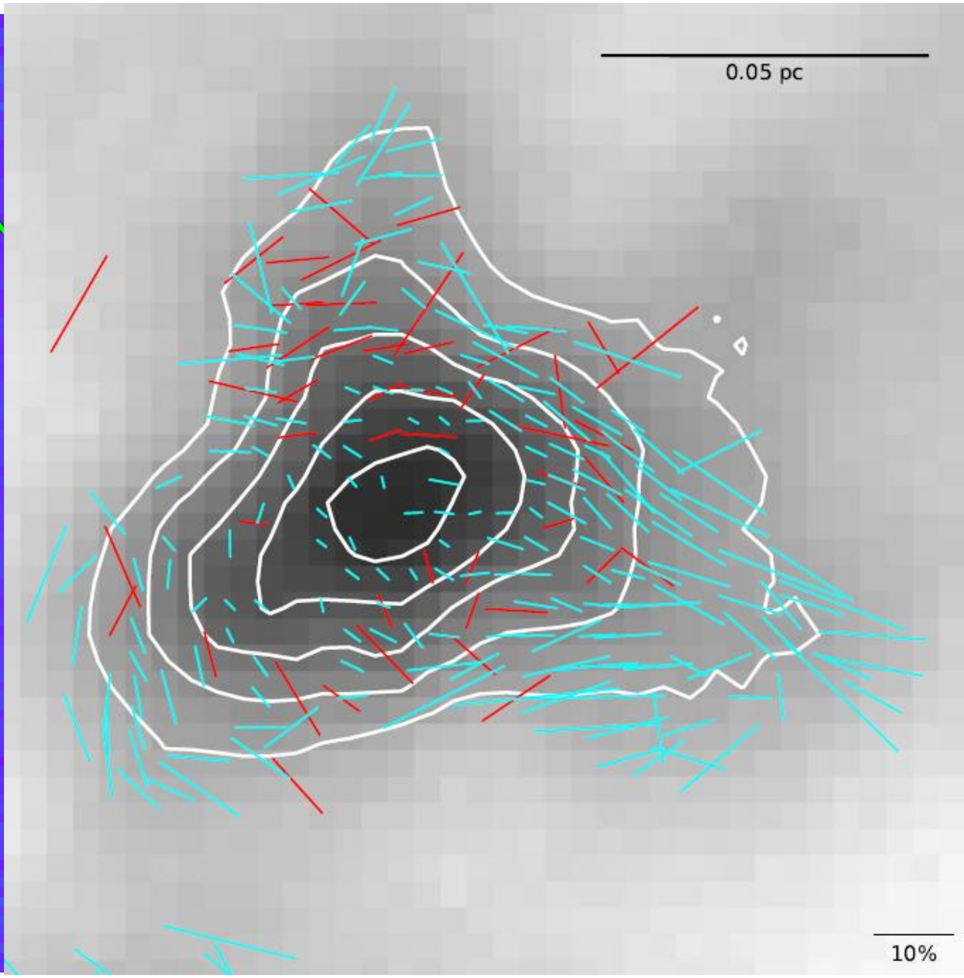

Left: Magnetic field orientation in the IC 5146 hub-filament structure.
Wang+ 2019

Right: Magnetic field orientation in the ρ Ophiuchus C clump.
Liu+ 2019

Published BISTRO Results

Region	Paper	Field strength	Criticality
Orion A	Pattle+ 2017	6.6 ± 4.7 mG	0.41
Perseus B1	Coudé+ 2019	120 ± 60 μG	3.0 ± 1.5
IC 5146	Wang+ 2019	0.5 ± 0.2 mG	1.3 ± 0.4
ρ Ophiuchus A	Kwon+ 2018	N/A	N/A
ρ Ophiuchus B	Soam+ 2018	630 ± 410 μG	1.6 ± 1.1
ρ Ophiuchus C	Liu+ 2019	~ 150 μG	~ 2
Messier 17	Pattle+ 2018	N/A	N/A

Criticality: $\lambda \sim 7.6 \times 10^{-21} \frac{N(H_2)}{B}$

…and more results coming soon!

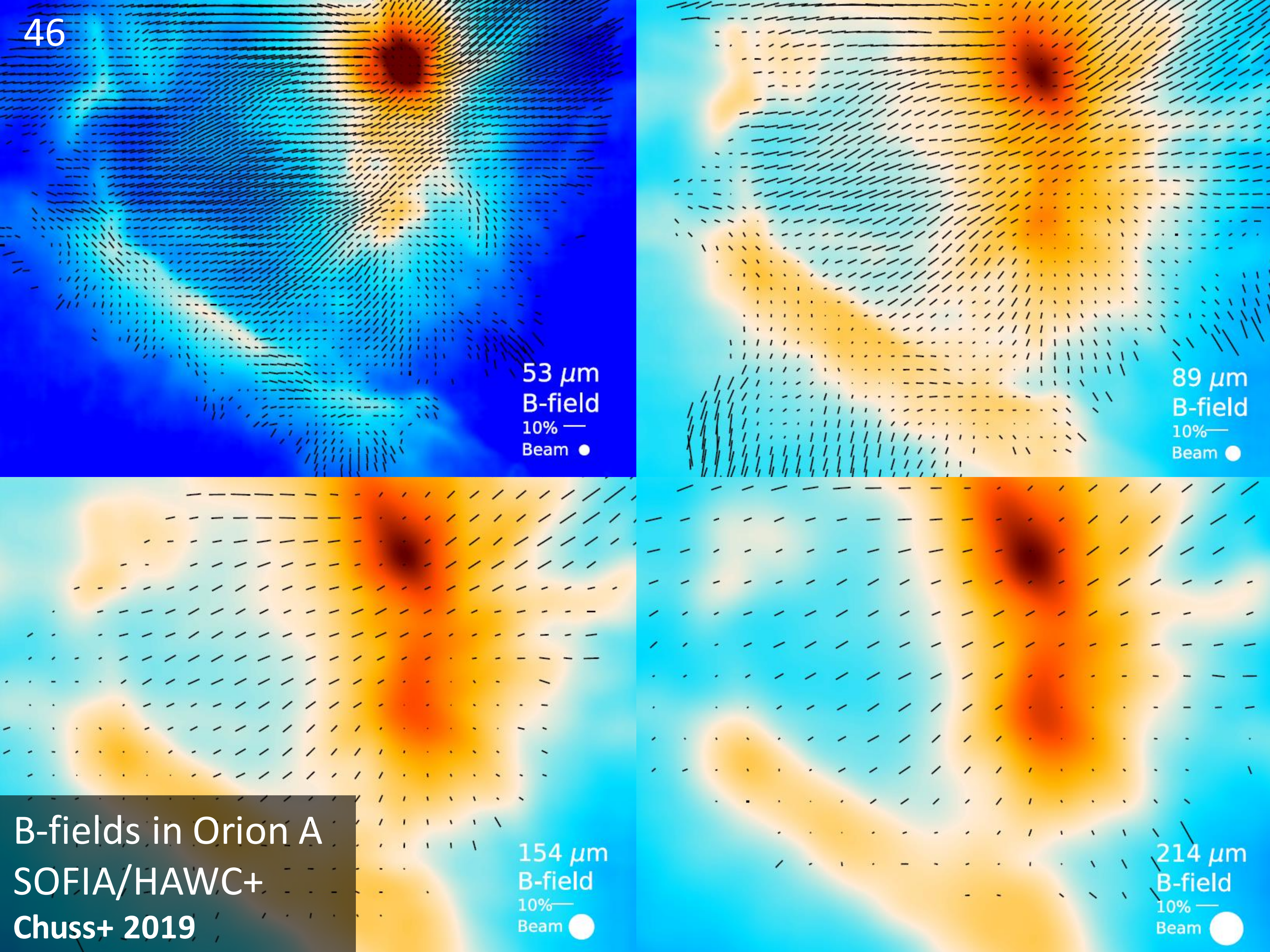

B-fields in Orion A
SOFIA/HAWC+
Chuss+ 2019

Magnetic Fields in Star-Forming Regions

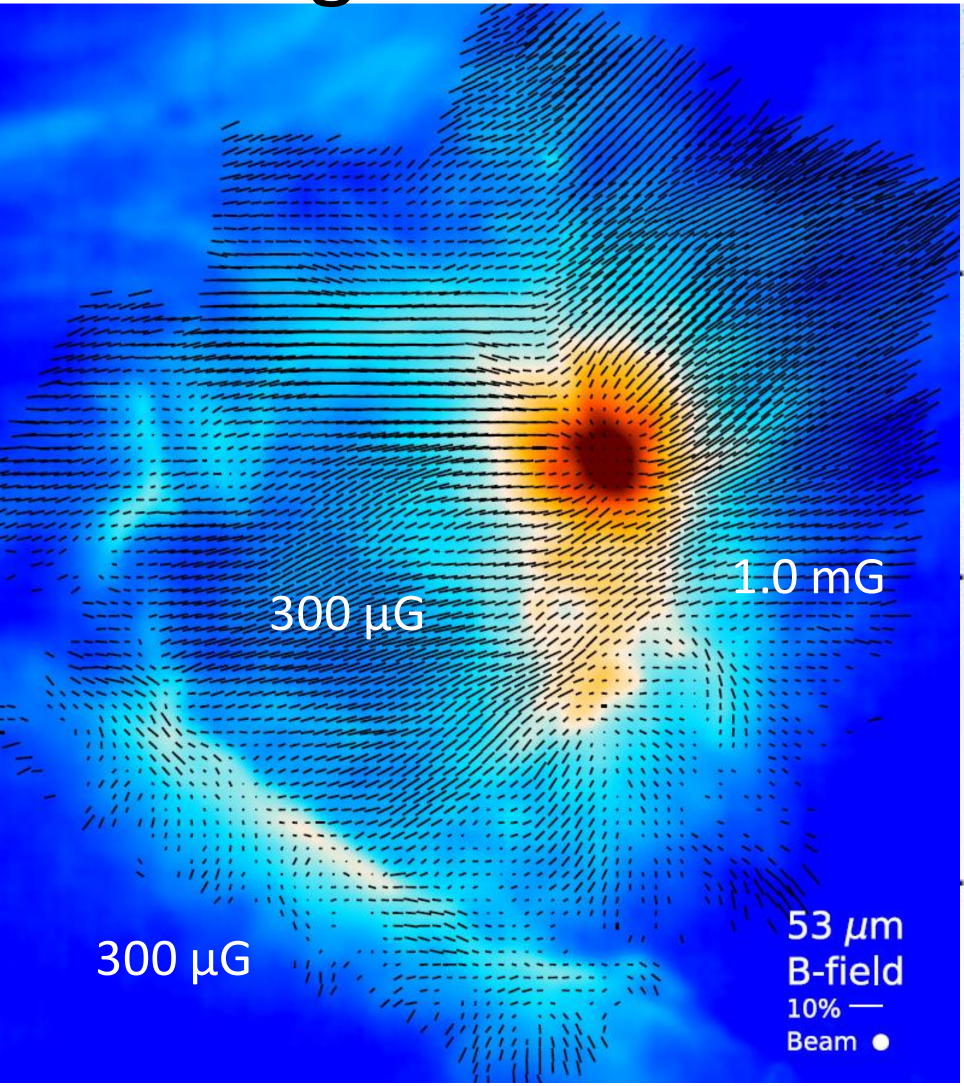

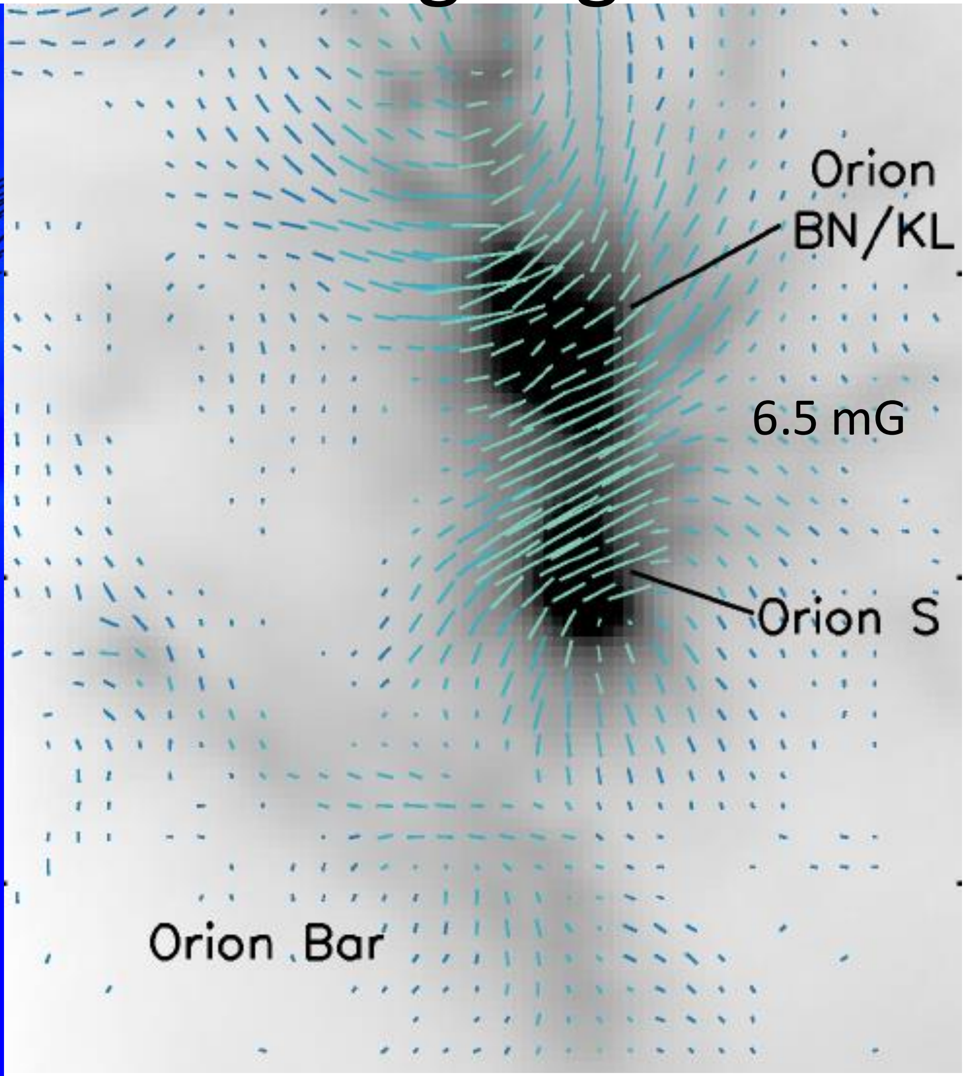

Left: 53 μm observations of Orion A. Magnetic field amplitude $B \sim 1.0$ mG.
Chuss+ 2019

Right: 850 μm observations of Orion A. Magnetic field amplitude $B \sim 6.5$ mG.
Pattle+ 2017

Magnetic Fields in Protostellar Cores

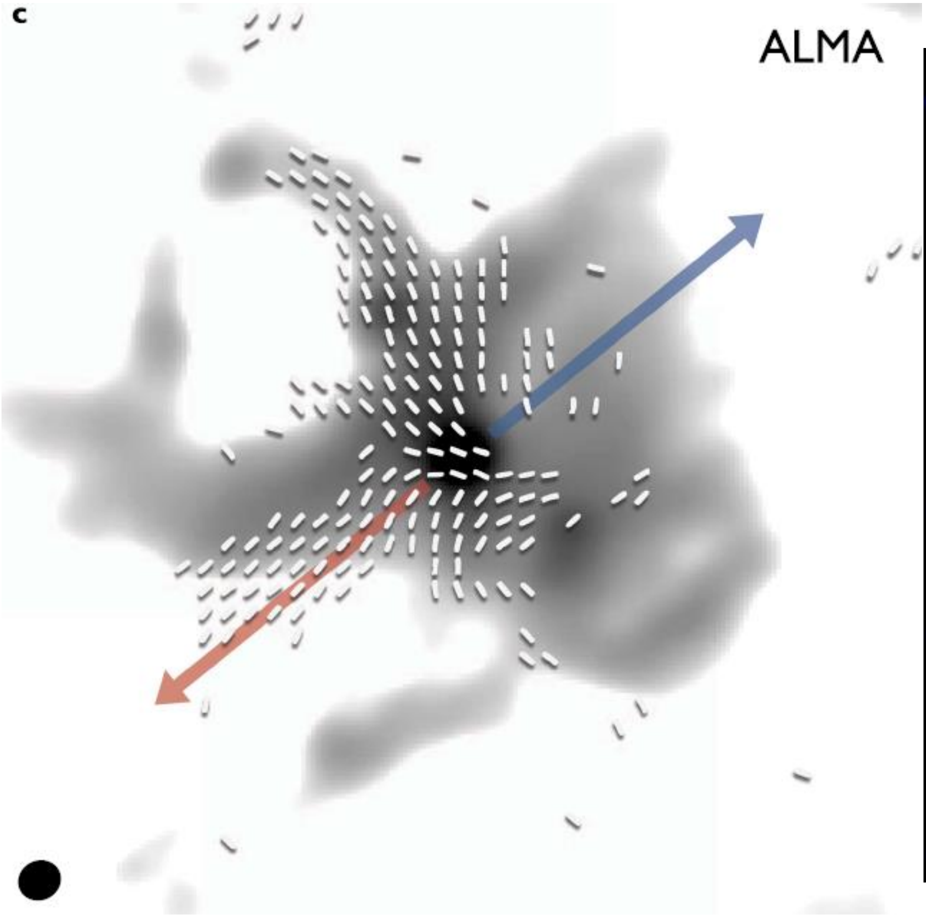

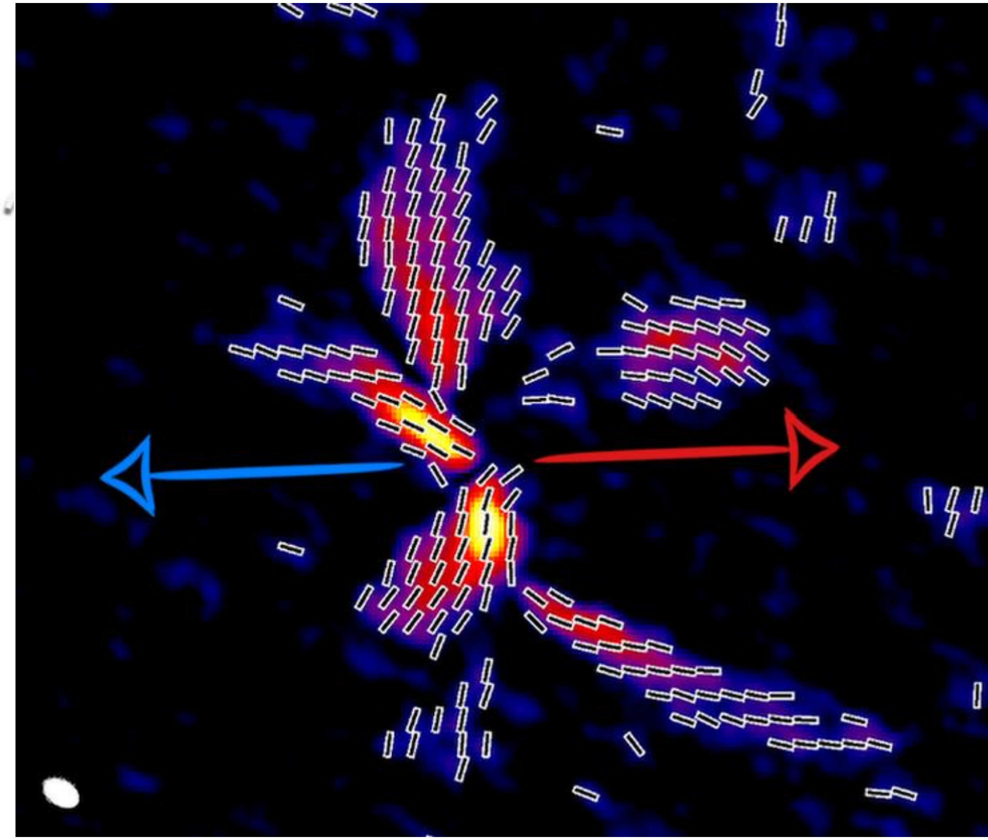

Left: Magnetic field orientation in the Ser-emb-8 protostellar core (Serpens). **Hull+ 2017**

Right: Magnetic field orientation in the nearby B335 protostellar core. **Maury+ 2018**

4. Testing Grain Alignment Mechanisms

The alignment efficiency of interstellar dust

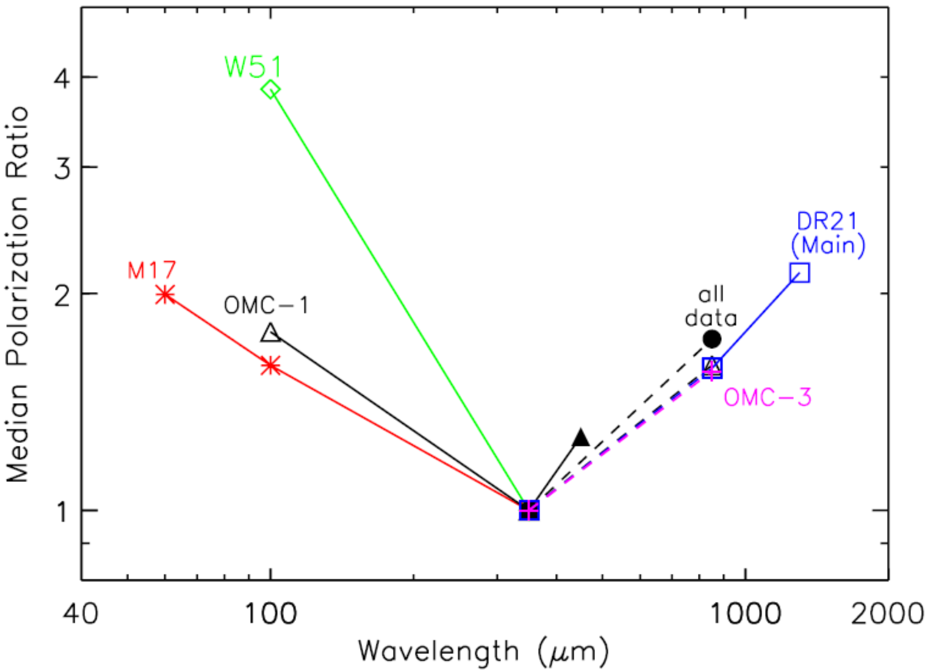

Left: Polarisation spectrum from **Vaillancourt & Matthews 2012**

- Grain alignment efficiency
  - Test for RAT theory
    - **Andersson+ 2015**
  - Environmental differences?
  - Dust composition

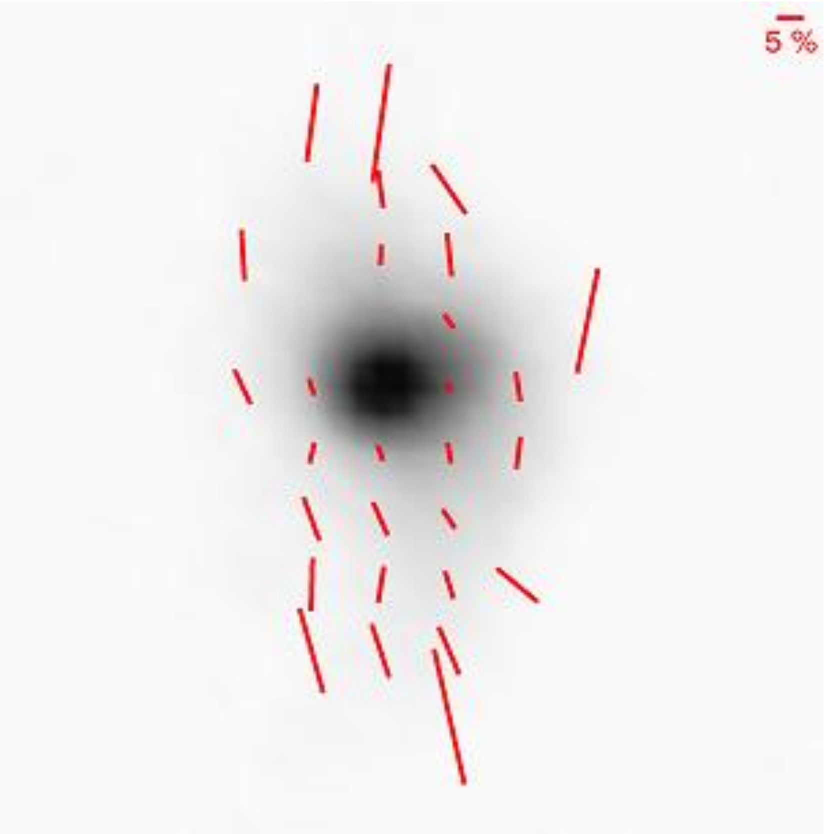

Right: POL-2 850 μm polarisation map of the CB 68 protostellar core

Multi-wavelengths Polarization

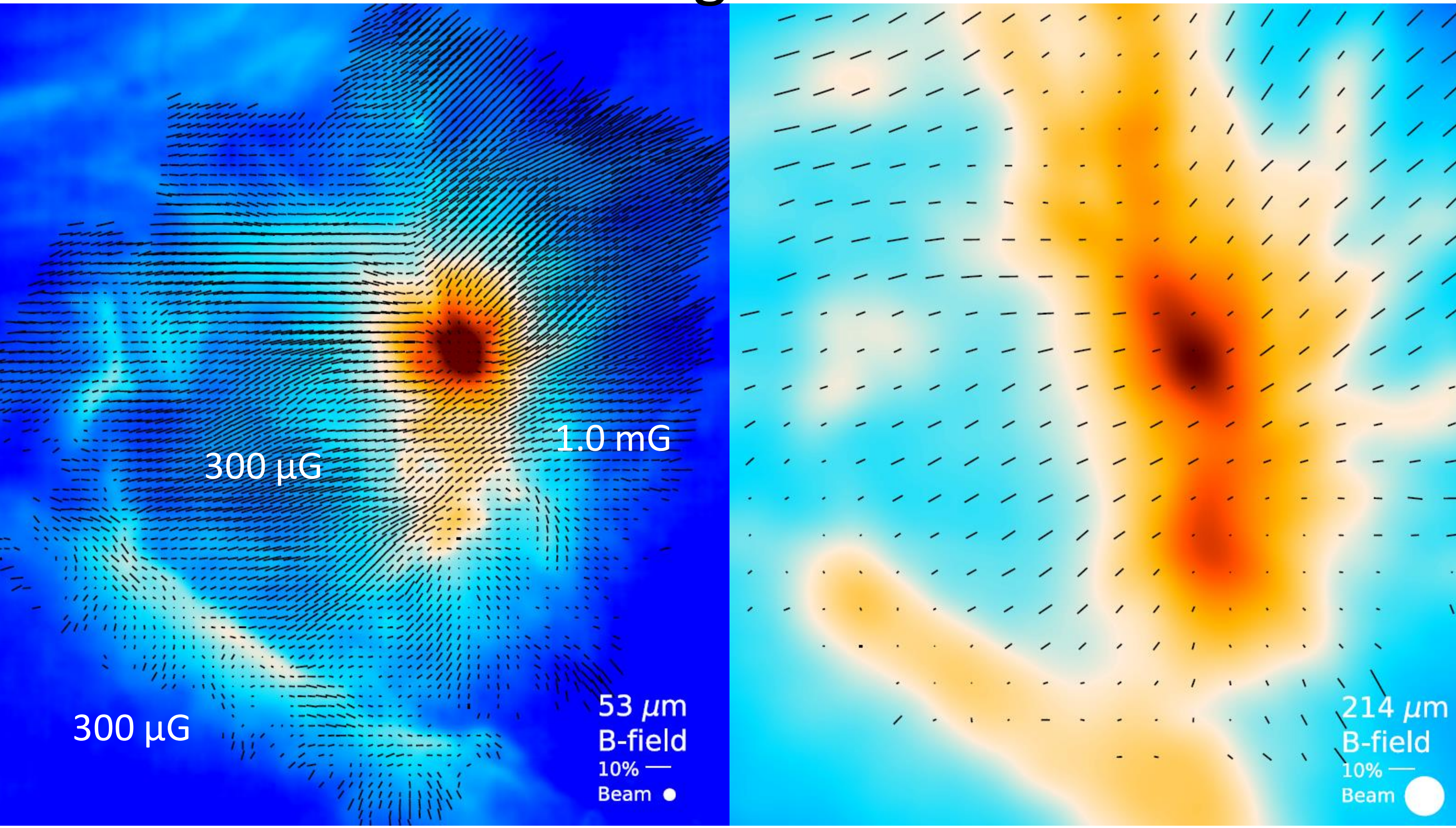

<u>Left</u>: 53 μm observations of Orion A. **Chuss+ 2019**

<u>Right</u>: 214 μm observations of Orion A. **Chuss+ 2019**

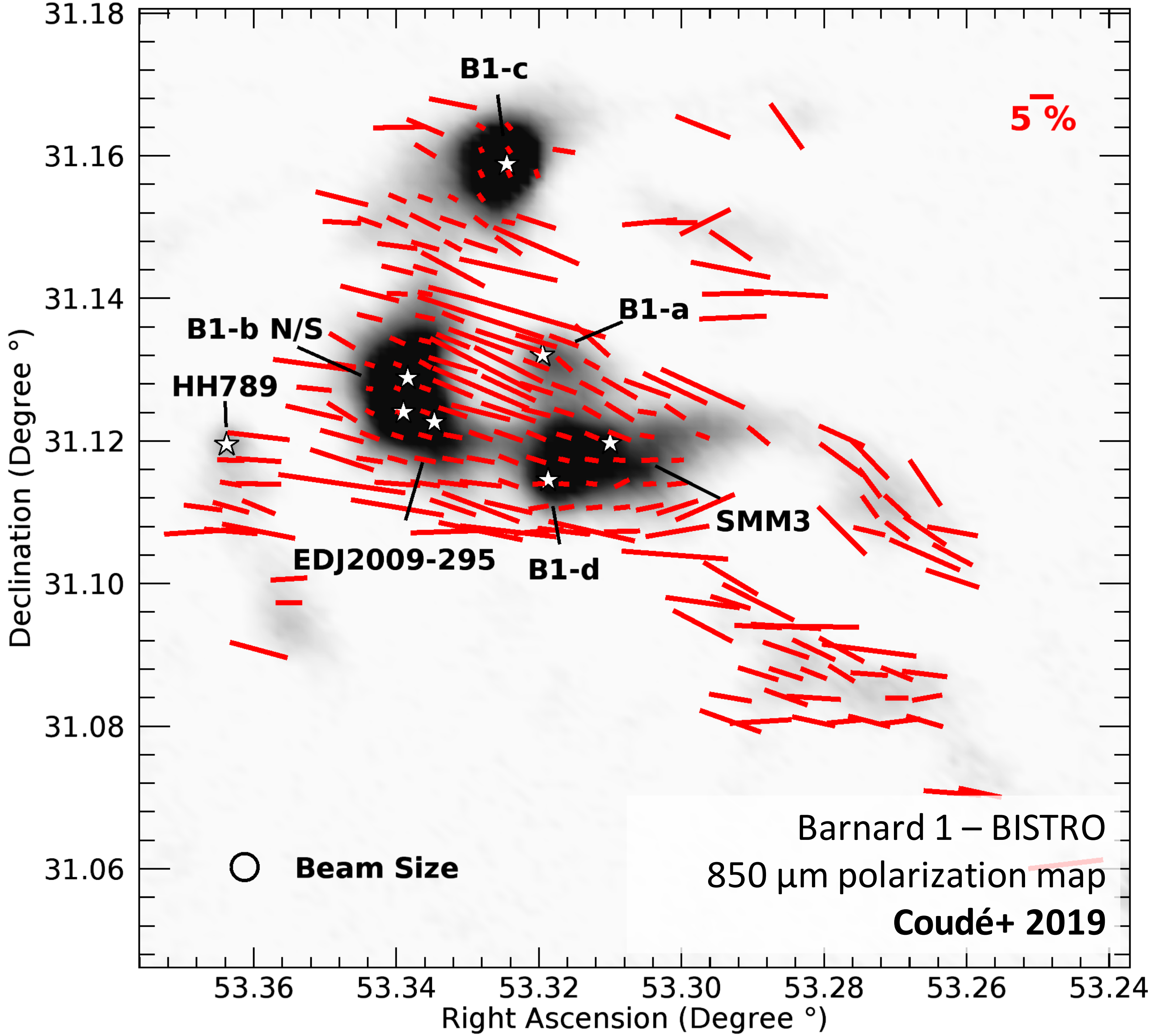

B1-c
5 %
B1-a
B1-b N/S
HH789
SMM3
EDJ2009-295
B1-d
Beam Size
Barnard 1 – BISTRO
850 µm polarization map
Coudé+ 2019
Declination (Degree °)
Right Ascension (Degree °)
31.18
31.16
31.14
31.12
31.10
31.08
31.06
53.36
53.34
53.32
53.30
53.28
53.26
53.24

53 Depolarization effects in molecular clouds

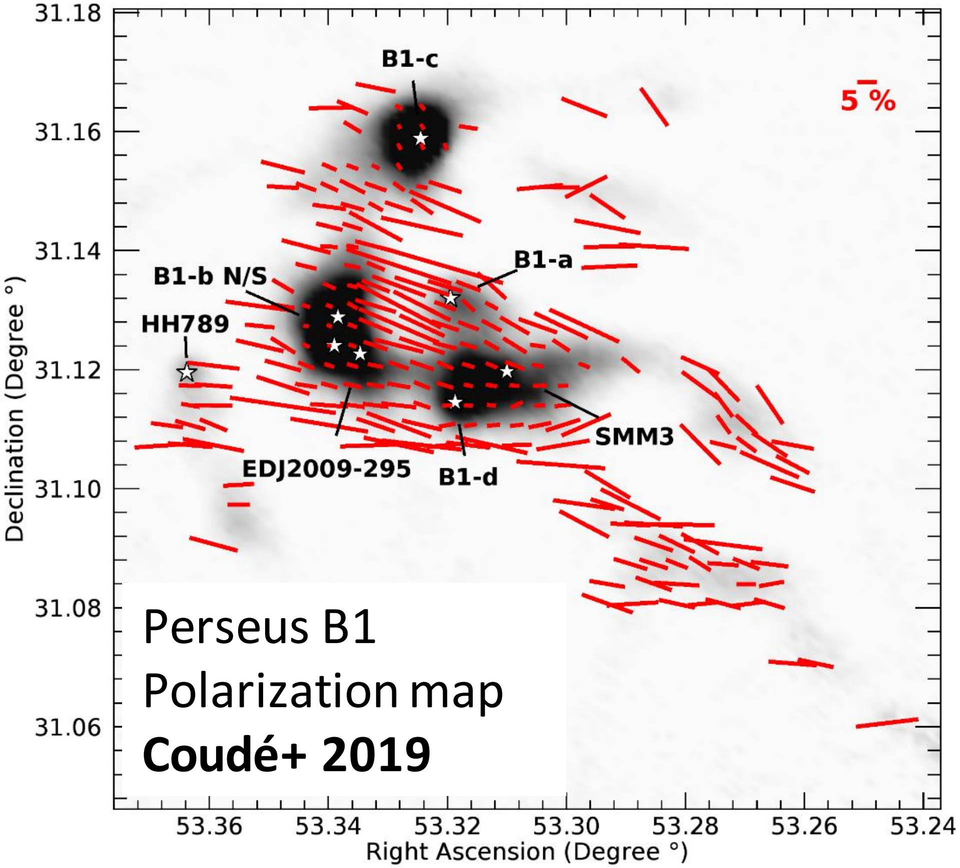

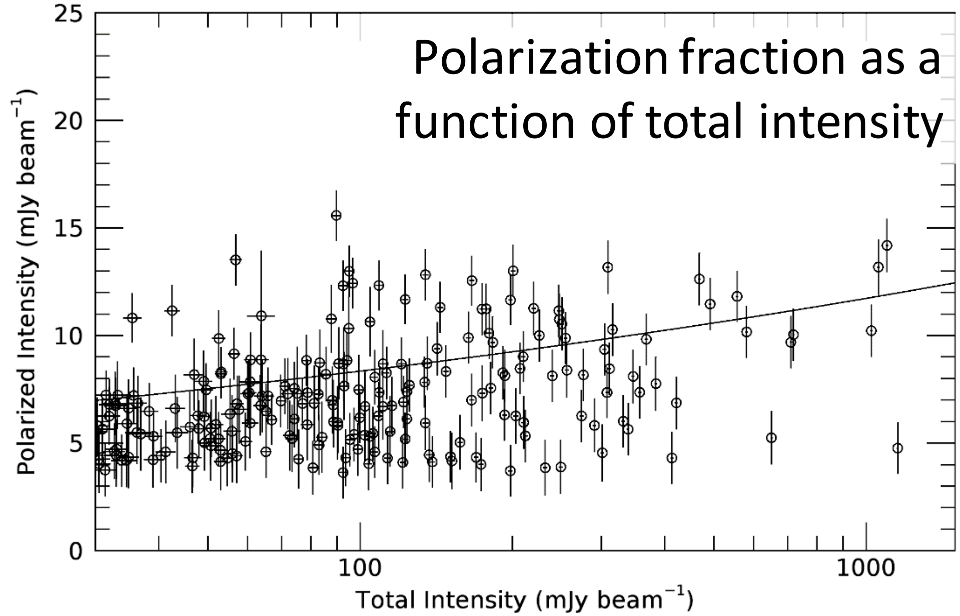

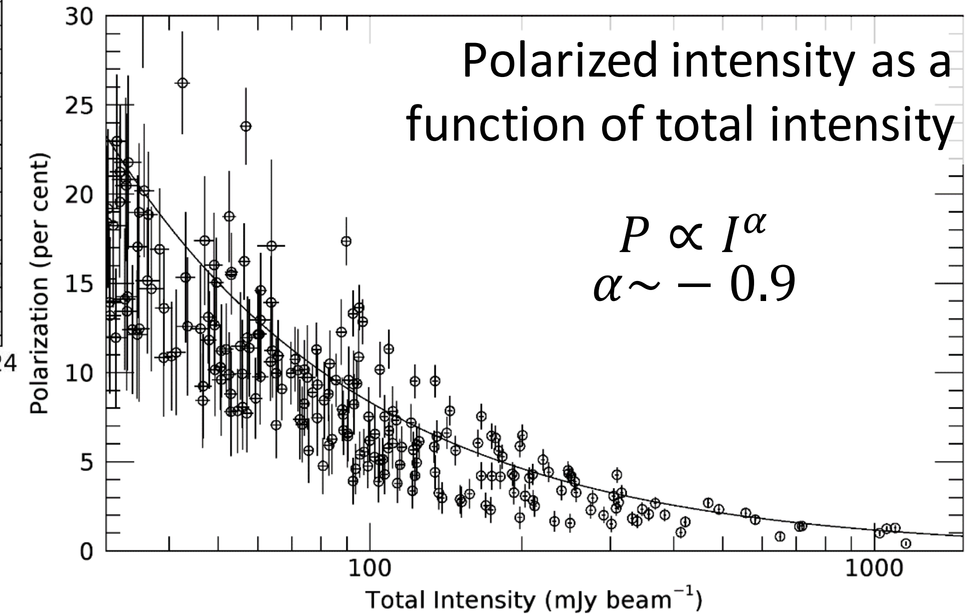

- Grain alignment efficiency
- Turbulent cells along line-of-sight
- Complex 3D field morphology
- ^{12}CO J=3-2 contamination

Depolarization effects in molecular clouds

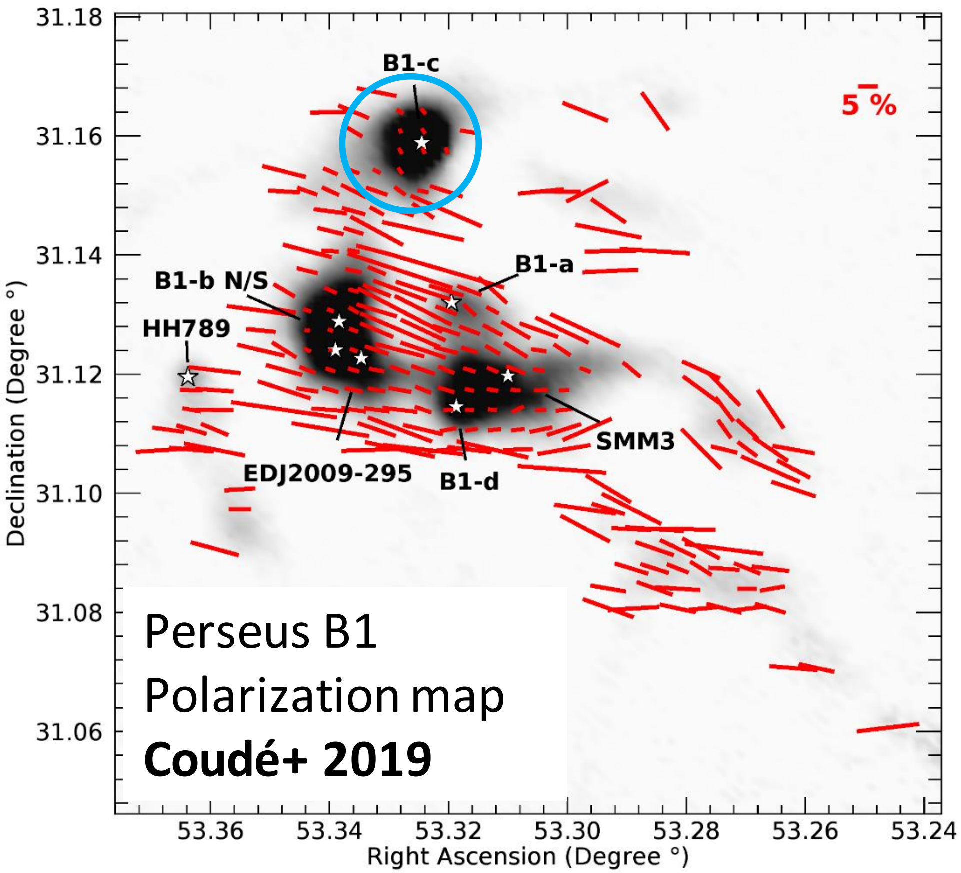

Perseus B1
Polarization map
Coudé+ 2019

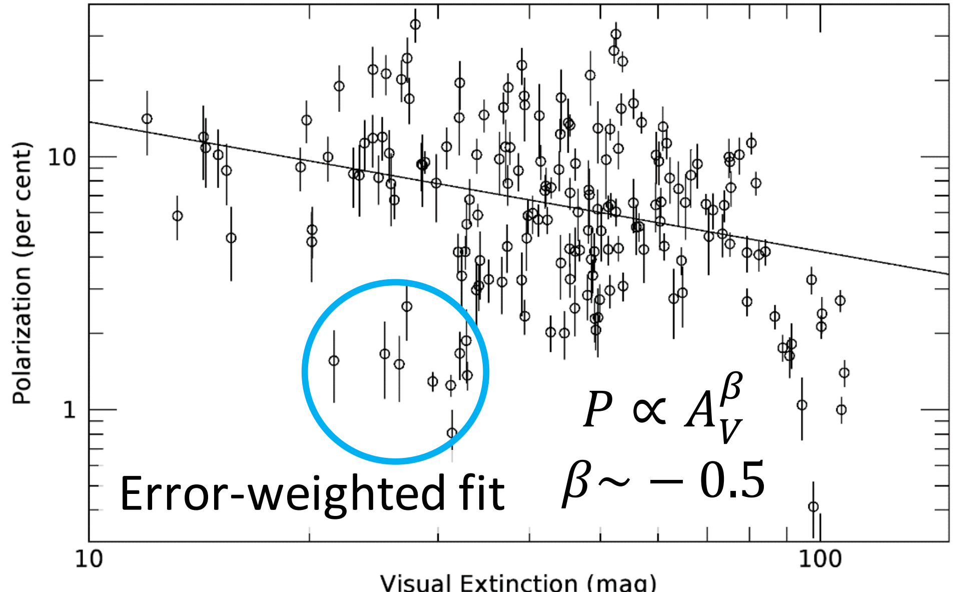

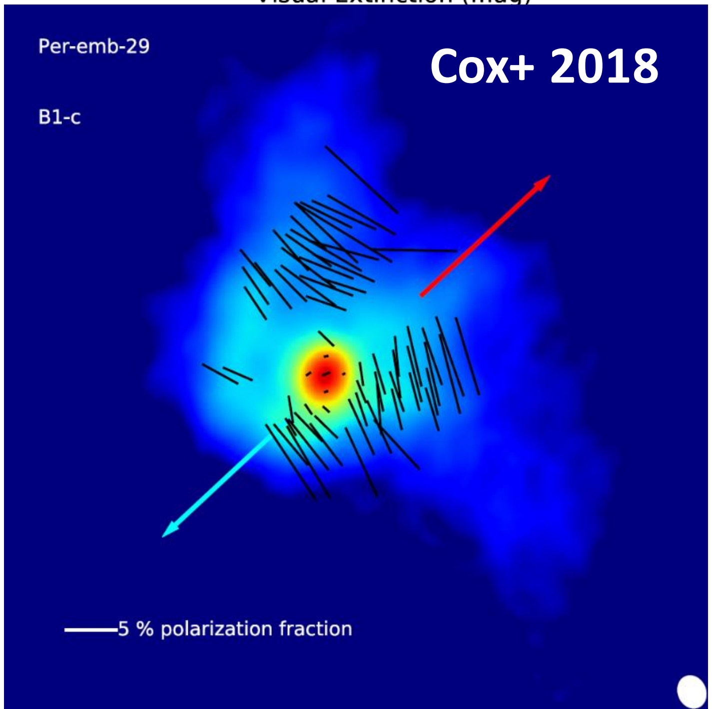

- Depolarization with extinction A_V
  - Test for radiative alignment
  - Opacity maps from **Chen+ 2016**

Conclusions

1. New age of far-infrared and submillimeter polarimetry
   - SOFIA, JCMT, ALMA, BLAST-TNG, and more!

2. Probing the dynamics of star formation
   - Magnetic field amplitude and criticality in star-forming regions
   - Field morphology, filaments, and outflows

3. Testing grain alignment mechanisms
   - Multi-wavelength and multi-scale polarimetry
   - Testing RATs in high extinction environments

Merci!
Thank you!
Mahalo!

References

- Andersson B.-G., Lazarian A. & Vaillancourt J.E. 2015, ARA&A, 53, 501
- André P. et al. 2010, A&A, 518, L102
- André P. et al. 2014, PPVI, 27
- Chandrasekhar S. & Fermi E. 1953, ApJ, 118, 113
- Chen M. C.-Y. et al. 2016, ApJ, 826, 95
- Chuss D. T. et al. 2019, ApJ, 872, 187
- Coudé S. et al. 2019, arXiv:1904.07221
- Cox E. G. et al. 2018, ApJ, 855, 92
- Crutcher R. M. et al. 2004, ApJ, 600, 279
- Drabek E. et al. 2012, MNRAS, 426, 23
- Draine B. T. & Lee H. M. 1984, ApJ, 285, 89
- Draine B. T. & Anderson N. 1985, ApJ, 292, 494
- Fissel L. M. et al. 2016, ApJ, 824, 134
- Franzmann E. L. & Fiege J. D. 2017, MNRAS, 466, 4592
- Friesen R. K. et al., 2017, ApJ, 843, 63
- Girart J. M., Rao R. & Marrone D. P. 2006, Science, 313, 812
- Harper D. A. et al. 2018, JAI, 7, 40008
- Holland J. W. et al. 2013, MNRAS, 430, 2513
- Houde M. et al. 2009, ApJ, 706, 1504
- Hull C. L. H. et al. 2017, ApJ, 847, 92
- Kataoka A., Machida M. N. & Tomisaka K. 2012, ApJ, 761, 40
- Kwon J. et al. 2018, ApJ, 859, 4
- Lazarian A. & Hoang T. 2011, ASPC, 449, 116
- Liu J. et al. 2019, arXiv:1902.07734
- Lazarian A. & Hoang T. 2007, MNRAS, 378, 910

References

- Machida M. N., Inutsuka S.-i. & Matsumoto T. 2008, ApJ, 676, 1088
- Matthews B. C. et al. 2006, ApJ, 652, 1374
- Matthews B. C. et al. 2009, ApJS, 182, 143
- Mathis J. S., Rumpl W. & Norsdsieck K. H. 1977, ApJ, 217, 425
- Maury A. J. et al. 2018, MNRAS, 477, 2760
- Pattle K. et al. 2017, ApJ, 846, 122
- Pattle K. et al. 2018, ApJL, 860, 6
- Sadavoy S. et al. 2012, A&A, 540, A10
- Salji C. et al. 2015, MNRAS, 449, 1782
- Soam A. et al. 2018, ApJ, 861, 65
- Stephens I. W. et al. 2017, ApJ, 851, 55
- Tomida K. et al. 2013, ApJ, 763, 6
- Tomisaka K. 2015, ApJ, 807, 47
- Wang J.-W. et al. 2019, ApJ, 876, 42
- Ward-Thompson D. et al. 2017, ApJ, 842, 66

Appendices

Orion A integral-shaped filament
Credit: ESA – *Herschel* Gould Belt Survey, **André+ 2010**

The SCUBA-2 Camera

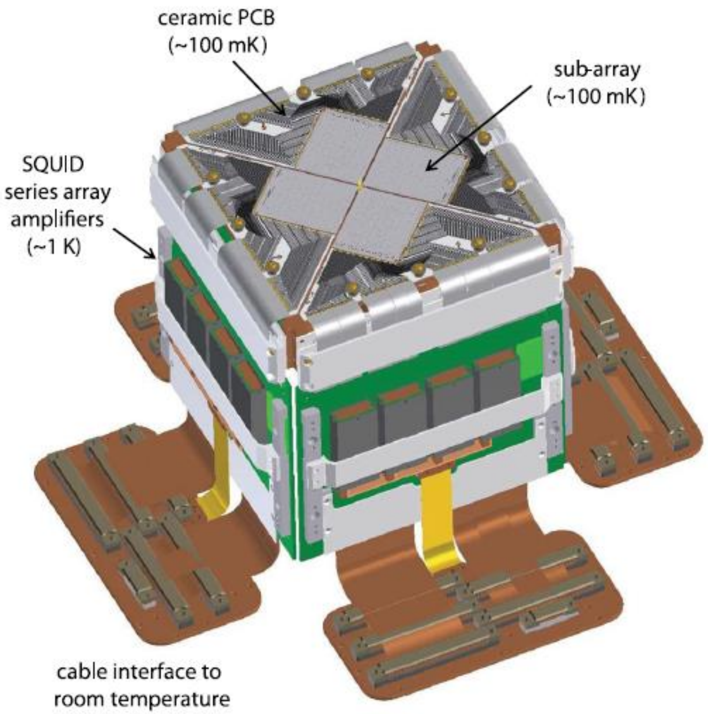

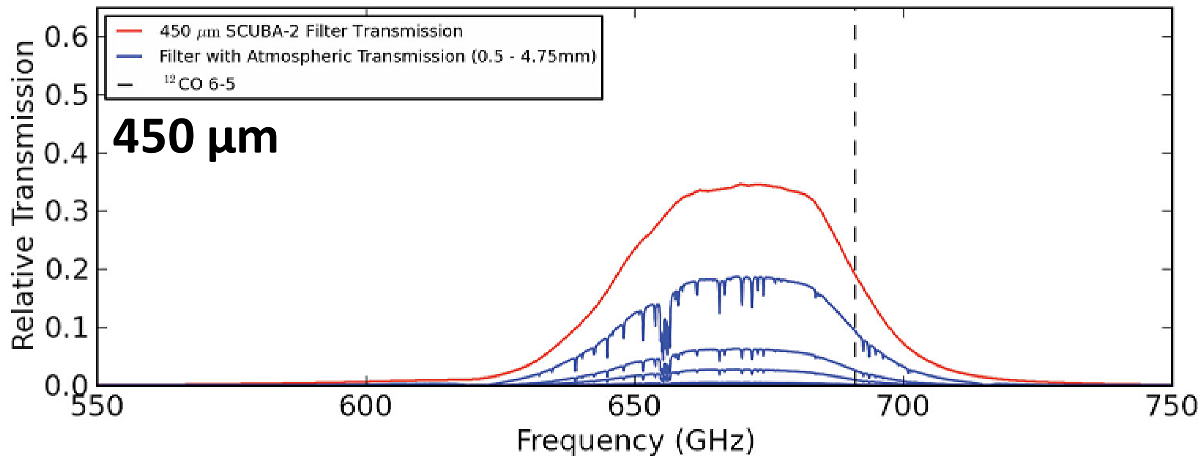

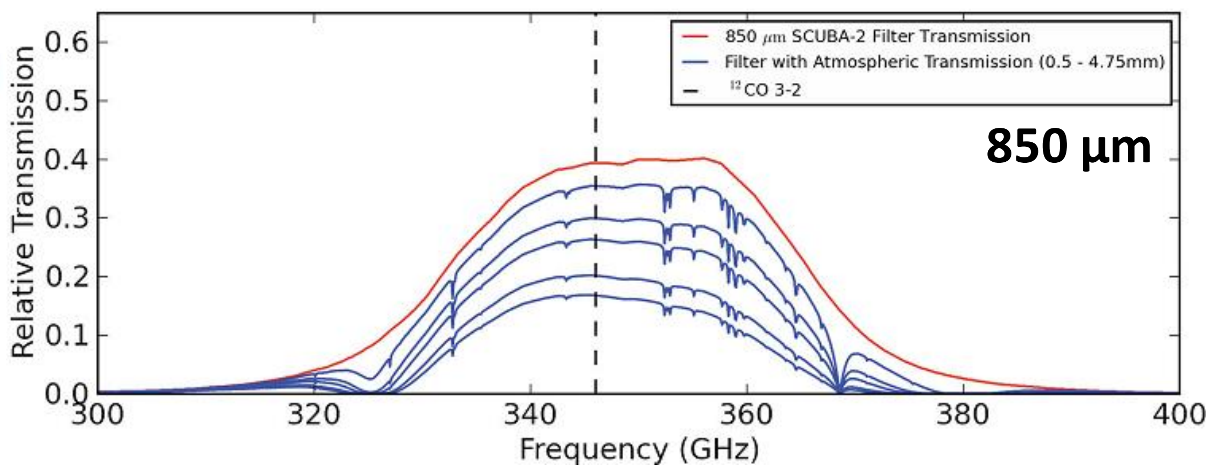

Left: SCUBA-2 detector array
Submillimetre Common-User Bolometer Array
Holland+ 2013

Right: Effective transmission of SCUBA-2
Drabek+ 2012

POL-2: The SCUBA-2 Polarimeter

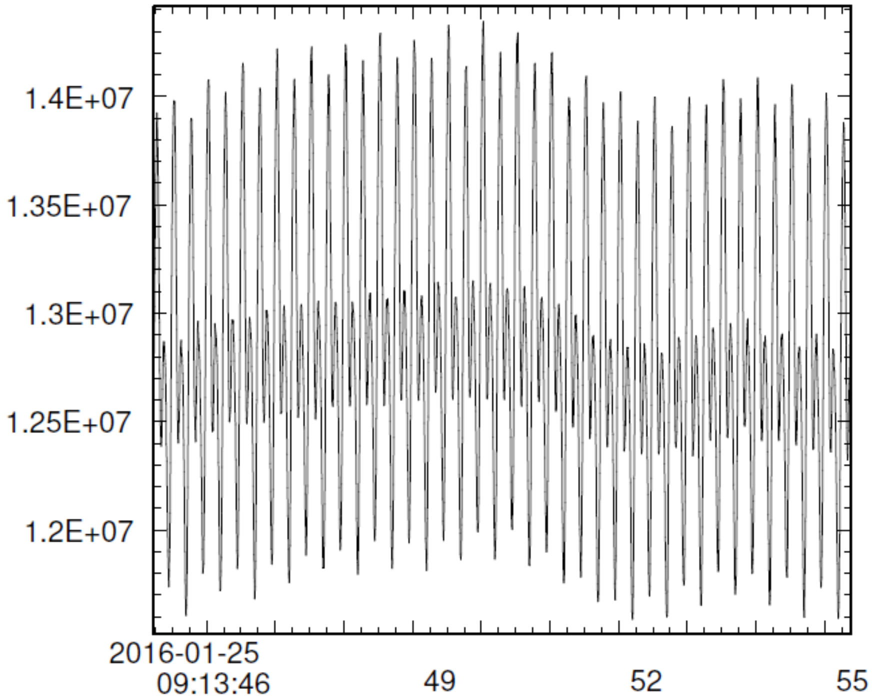

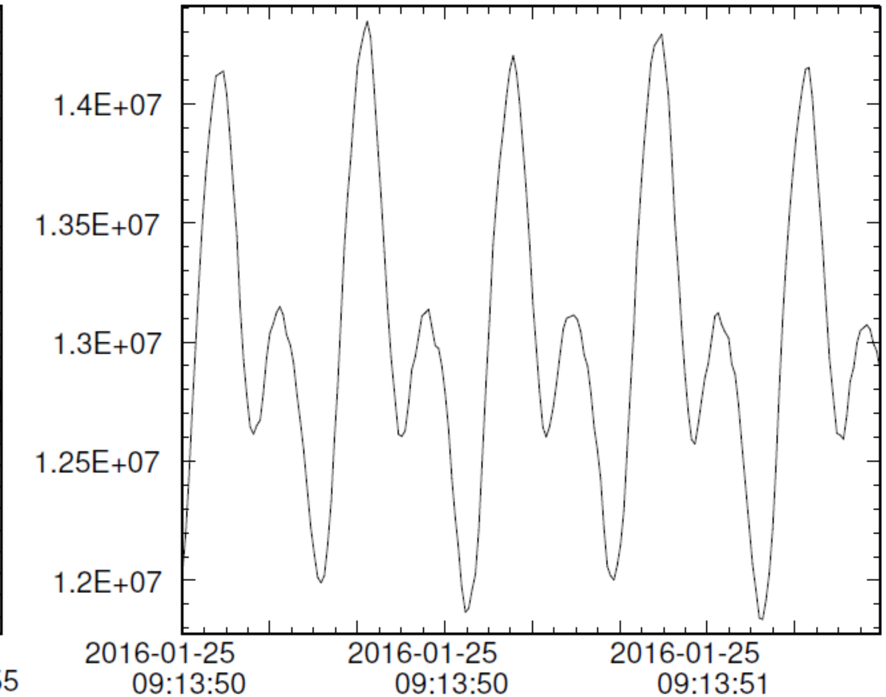

Top: Typical modulated signal produced by POL-2
Credit: EAO/David Berry

Bottom: Picture of the POL-2 polarimeter
Credit: EAO/Pierre Bastien

- Rotating half-wave plate and analyzer
  - 2 Hz rotation
  - 8 Hz polarized astronomical signal
  - ∼190 Hz sampling

SOFIA says...

#NASA747

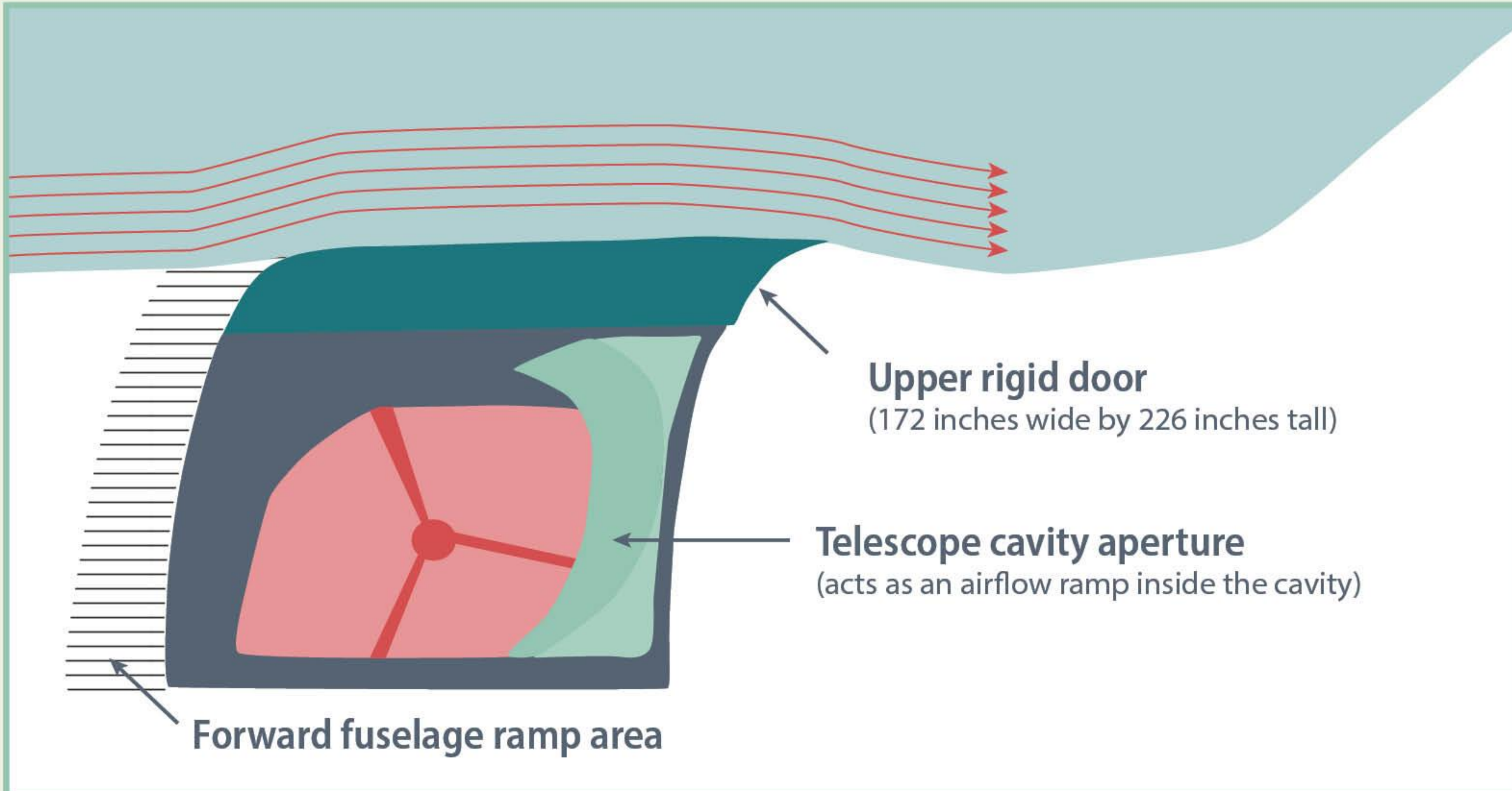

"Airflow travels up and over the telescope cavity, guided by the forward fuselage ramp. The aperture directs away most of the air trying to enter the cavity."

Comparison with SCUPOL

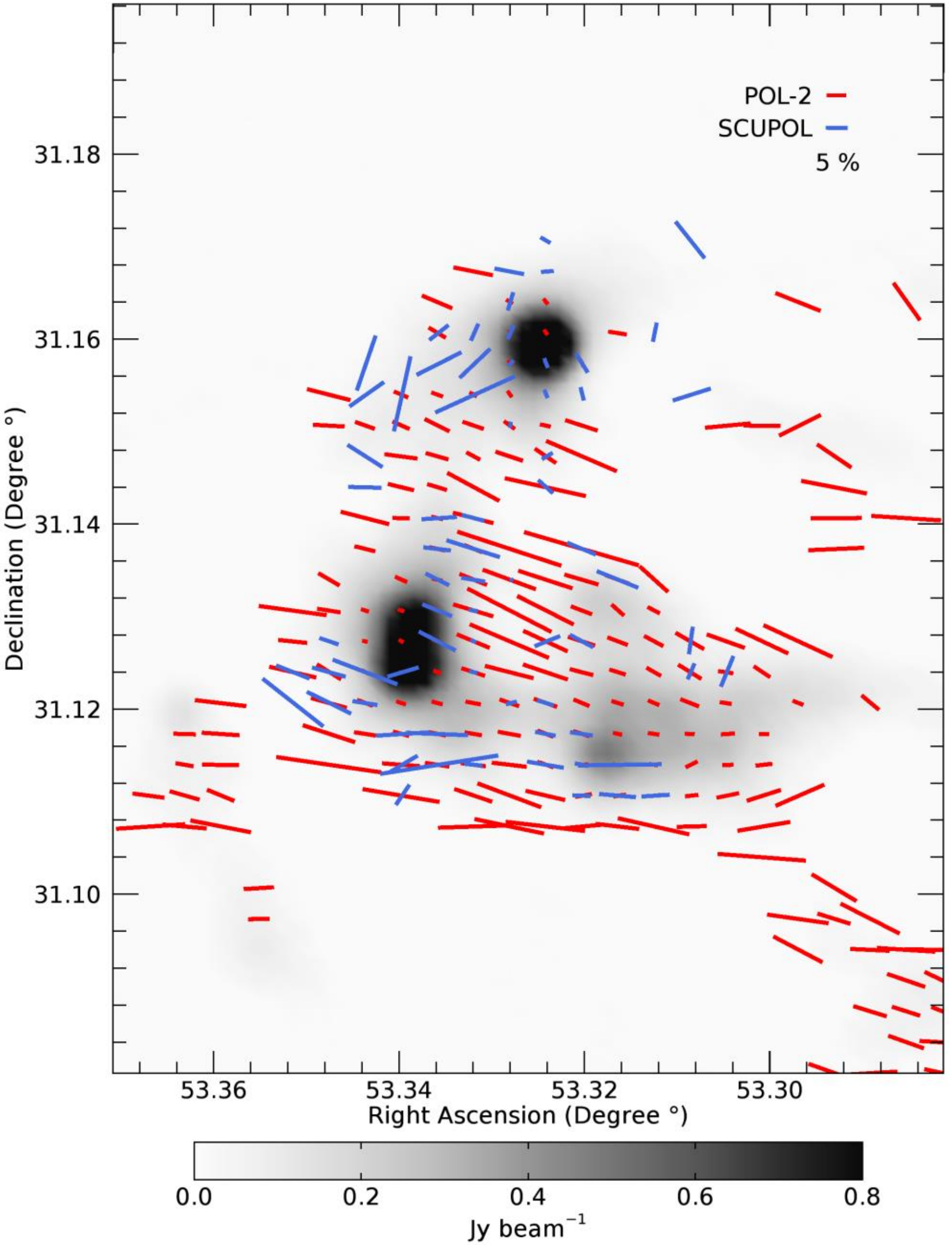

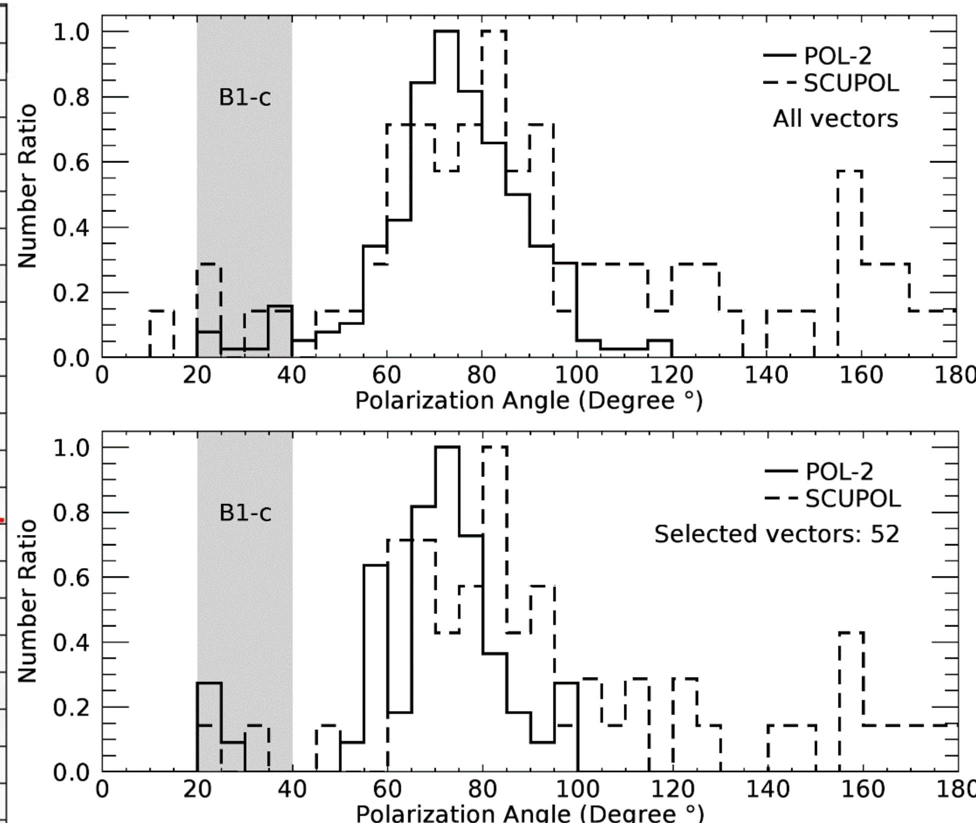

Right: Histograms of polarization angles

Top: All vectors

Bottom: Overlapping vectors

Left: Comparison with the SCUPOL Legacy Catalog - **Matthews+ 2009**

Comparison with SCUPOL

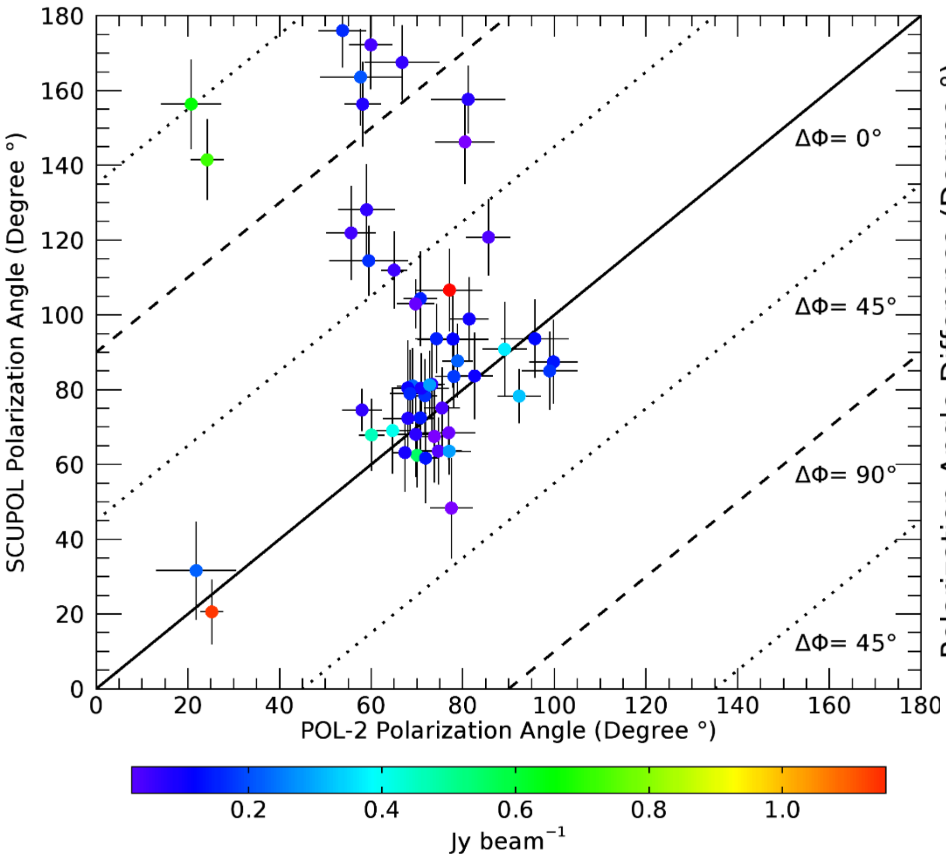

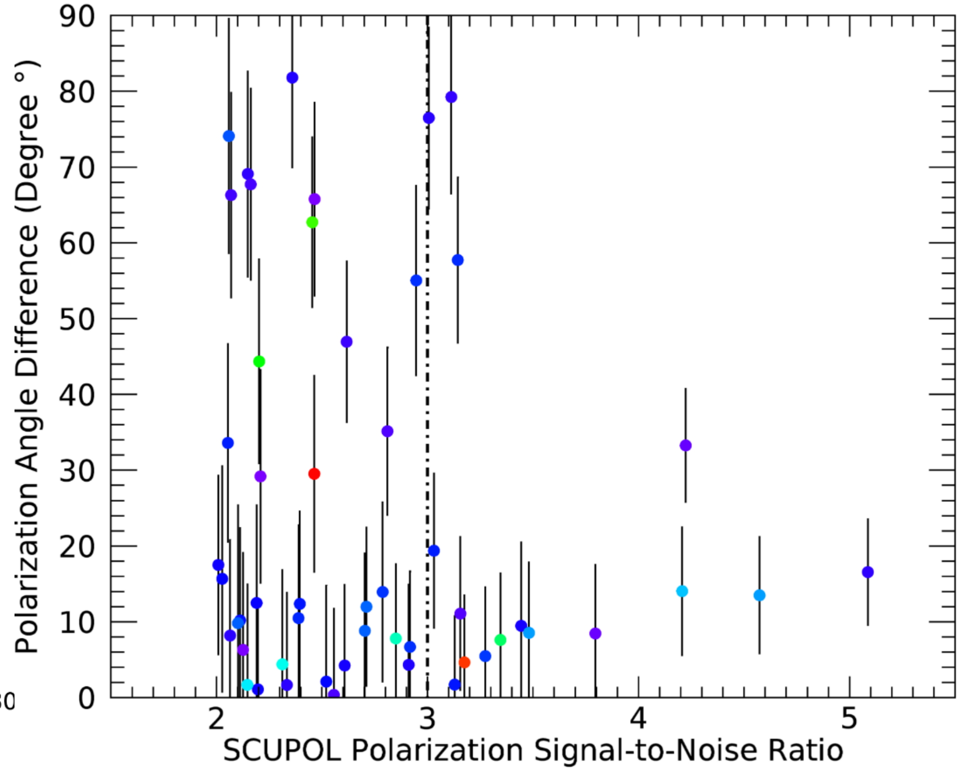

<u>Left</u>: Comparison between overlapping POL-2 and SCUPOL vectors

<u>Right</u>: Difference as a function of SCUPOL Signal-to-Noise ratio